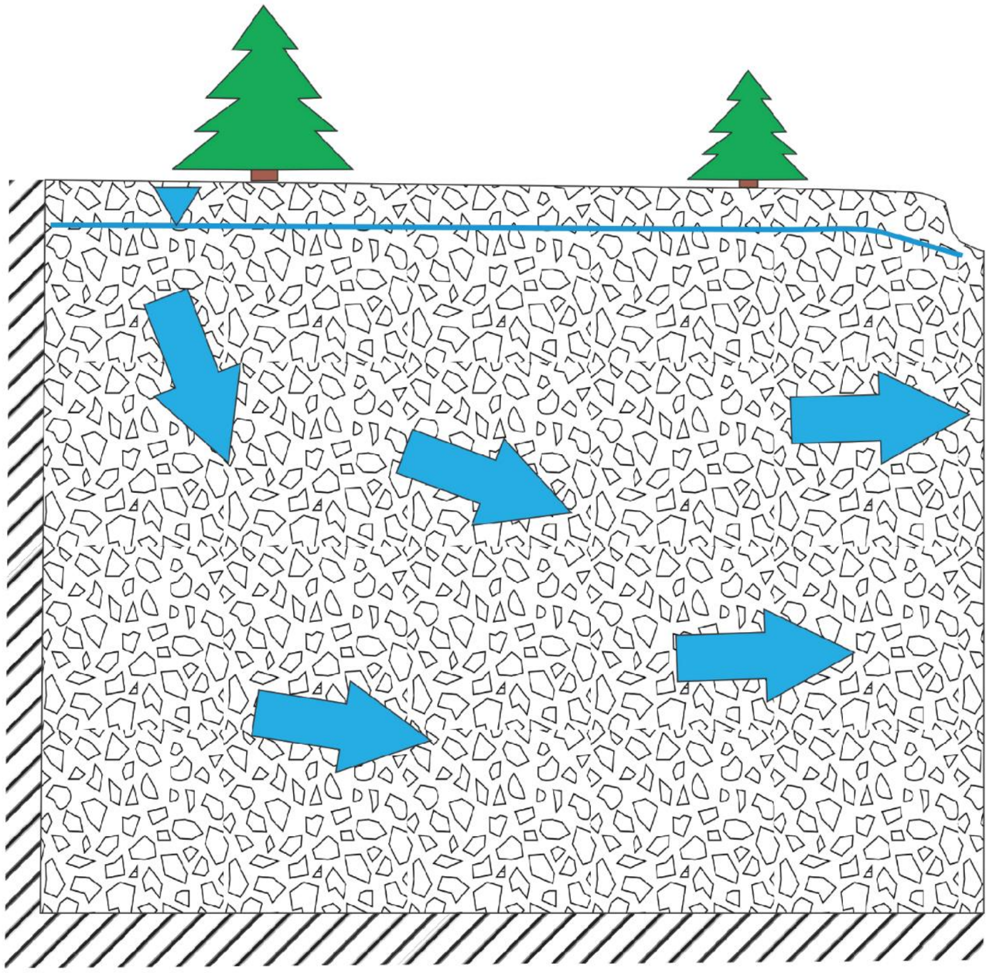

Groundwater Velocity

J.F. Devlin

THE GROUNDWATER PROJECT

Groundwater Velocity

The Groundwater Project

J.F. Devlin
Professor,
Department of Geology,
University of Kansas
Lawrence, Kansas, USA

Groundwater Velocity

The Groundwater Project
Guelph, Ontario, Canada

Published by the Groundwater Project, Guelph, Ontario, Canada, 2020.

Devlin, J.F.
Groundwater Velocity / J.F. Devlin - Guelph, Ontario, Canada, 2020.
64 pages

ISBN: 978-1-77470-000-6

Please consider signing up to the Groundwater Project mailing list and stay informed about new book releases, events and ways to participate in the Groundwater Project. When you sign up to our email list it helps us build a global groundwater community. Sign-up↗.

Citation: Devlin, J.F., 2020, Groundwater Velocity↗. The Groundwater Project, Guelph, Ontario, Canada.

Domain Editors: John Cherry and Eileen Poeter
Topic Leads: Eileen Poeter and John Cherry

Cover Image: J.F. Devlin

Dedication

To my wife Frances and daughter Jessica who were with me when I first heard the call to pull on the thread that became this book. Their patience, humor and companionship made the years of developing the idea(s) presented here fly by.

Table of Contents

The Groundwater Project Foreword

The United Nations Water Members and Partners establish their annual theme a few years in advance. The theme for World Water Day of March 22, 2022, is “Groundwater: making the invisible visible.” This is most appropriate for the debut of the first Groundwater Project (GW-Project) books in 2020, which have the goal of making groundwater visible.

The GW-Project, a non-profit organization registered in Canada in 2019, is committed to contribute to advancement in education and brings a new approach to the creation and dissemination of knowledge for understanding and problem solving. The GW-Project operates the website https://gw-project.org↗ as a global platform for the democratization of groundwater knowledge and is founded on the principle that:

“Knowledge should be free and the best knowledge should be free knowledge.” Anonymous

The mission of the GW-Project is to provide accessible, engaging, high-quality, educational materials, free-of-charge online in many languages, to all who want to learn about groundwater and understand how groundwater relates to and sustains ecological systems and humanity. This is a new type of global educational endeavor in that it is based on volunteerism of professionals from different disciplines and includes academics, consultants and retirees. The GW-Project involves many hundreds of volunteers associated with more than 200 hundred organizations from over 14 countries and six continents, with growing participation.

The GW-Project is an on-going endeavor and will continue with hundreds of books being published online over the coming years, first in English and then in other languages, for downloading wherever the Internet is available. The GW-Project publications also include supporting materials such as videos, lectures, laboratory demonstrations, and learning tools in addition to providing, or linking to, public domain software for various groundwater applications supporting the educational process.

The GW-Project is a living entity, so subsequent editions of the books will be published from time to time. Users are invited to propose revisions.

We thank you for being part of the GW-Project Community. We hope to hear from you about your experience with using the books and related material. We welcome ideas and volunteers!

The GW-Project Steering Committee

December 2020

Foreword

Groundwater velocity is a fundamental and important parameter in groundwater science but often our treatment of it is cavalier. This is particularly so when we sacrifice accuracy and precision for the convenience offered by Darcy's Law. We do this in full knowledge of the large, well-known uncertainties that come from using estimates of hydraulic conductivity and hydraulic gradient to obtain the Darcy flux, then dividing by the bulk effective porosity. Even where no site-specific measurements of any of these parameters have been made, "guesstimates" of the parameter values are used to estimate a velocity value that can seem to satisfy the need. This approach has been useful for solving some groundwater problems, but is not the most desirable approach for cases in which velocity is a pivotal factor – a common occurrence in contaminant investigations.

In addition to the high uncertainty of the Darcy-based approach, a velocity value determined this way has inherent spatial and temporal scales that can be inappropriate for the problem at hand. These limitations might be overcome by conducting tracer tests across an entire study area but doing so requires multiple monitoring points and typically is fraught with difficulty. Of greater value are tracer tests conducted at smaller scales, particularly in individual monitoring wells or boreholes. A method for this, known as borehole dilution, appeared in the literature in the 1940's and was expanded on in publications in the 1950's, but was largely ignored in groundwater science. With the great expansion of attention to groundwater contamination in the late 20th and early 21st century, other approaches for measurement of velocity in single boreholes have been developed. The overall technology of velocity measurement has matured from a research activity to one that is ready for general use in solving diverse groundwater problems.

This book is the first of its kind in the groundwater education literature. Many of the single borehole methods, and consideration of Darcy velocity in the larger framework of velocity measurement, are examined in this book.

The author, Dr. J.F. Devlin, a professor at the University of Kansas, in the USA, has been at the forefront of development and testing of multiple methods for velocity measurement and has broad experience in applying this technology in a variety of groundwater conditions. With the publication of this book, our deficient respect for groundwater velocity as one of the key parameters in groundwater science can come to an end.

John Cherry, The Groundwater Project Leader

Guelph, Ontario, Canada, December 2020

Preface

In 1998 I was involved in a project that sequenced *in situ* remediation technologies to treat a plume of contaminated groundwater consisting of hydrocarbons and chlorinated solvents. An anaerobic treatment zone relying on zero-valent-iron was placed in the ground and followed by an aerobic biosparge zone. Laboratory work was undertaken to carefully measure the chemical transformation rates and sorption coefficients, as well as evaluating biodegradation rates and volatilization. Flow was directed through a funnel and gate system in a highly controlled fashion, with monitoring points and piezometers placed to maximize the characterization efforts. The treatment system was designed with a factor of safety that should have ensured that no anaerobically degradable substances passed into the downstream aerobic treatment zone. Nonetheless, the lesser chlorinated compounds, cis 1,2 DCE and vinyl chloride passed through the zero-valent-iron zone and into the aerobic zone. Why did this happen? Was the problem with the estimated transformation rates or did the water find preferred pathways through the iron that reduced the residence time of contaminants in the iron? Follow up laboratory work found plausible chemical reasons for the breakthrough of contaminants, but tracer tests and Darcy calculations were unable to satisfactorily rule out physical flow contributions to the breakthrough. The failure of the hydrogeological portion of this assessment was both surprising and disturbing. It ignited an interest in alternative methods and technologies for measuring groundwater velocity. Apparently, this experience — or the thinking it inspired — was not unique. Over the past couple of decades, a substantial and growing literature has appeared that offers alternatives for velocity estimation. Some of the methods represent brand new approaches while others are modifications of earlier ideas; some methods have gained increasing attention since their introduction and others have gone dormant. The lesson here is that researchers and practitioners have increasingly recognized the importance of groundwater velocity and the limitations of the conventional methods for its estimation. The goal of this book is to compile the reasons for hydrogeologists to consider alternative methods of groundwater velocity measurement, and to present a subset of the technologies that have gained attention through the years. Through the presentation of this material, it is hoped that both experienced and upcoming hydrogeologists may begin to explore the insights that the novel velocity measurements can offer, and perhaps themselves be inspired to imagine new and better ways to make these measurements.

Acknowledgements

This book owes its existence primarily to the persuasiveness of John Cherry, and the always penetrating yet supportive editing he and Eileen Poeter provided. The technical accuracy, readability of the work, and effectiveness of the exercises was also reviewed by several graduate students working in the Devlin group, including Trevor Osorno, Bryan Heyer, Allison Cormican, and Matt Jones.

The thorough and useful reviews of and contributions to this book by the following individuals is gratefully acknowledged:

- Peter Kitanidis, Professor, of Civil and Environmental Engineering, Stanford University, California, USA;
- Harald Klammler, Department of Civil & Coastal Engineering, University of Florida, Florida, USA;
- Mike Annable, Professor, Department of Civil & Coastal Engineering, University of Florida, Florida, USA;
- Peter Bennett, AMEC Geomatrix, 2101 Webster Street, 12th Floor, Oakland, California, USA; and,
- Vitaly Zlotnik, Professor Emeritus, University of Nebraska, Lincoln, Nebraska, USA.

I am grateful for Amanda Sills' oversight of this book and to Elhana Dyck for copyediting, both of the Groundwater Project, Guelph, Ontario, Canada. I thank Eileen Poeter (Colorado School of Mines, Golden, Colorado, USA) for copyediting, layout editing and production of this book.

1 Introduction

The word 'velocity' is a familiar one in the public lexicon. It brings to mind a baseball flying past a swinging bat, or a car hurtling down the highway. For most people, velocity is synonymous with 'speed'. However, for those in the sciences, the word velocity contains two important components: speed, as alluded to above, and the direction of movement. For those who study groundwater, both of these quantities are conveniently available through the application of Darcy's Law (discussed in depth in the following section), which relates flow rate to measurable physical characteristics of aquifers and dates back to 1856. However, though Darcy's Law is widely used to estimate groundwater velocity, it is only one of several methods currently available (Figure 1).

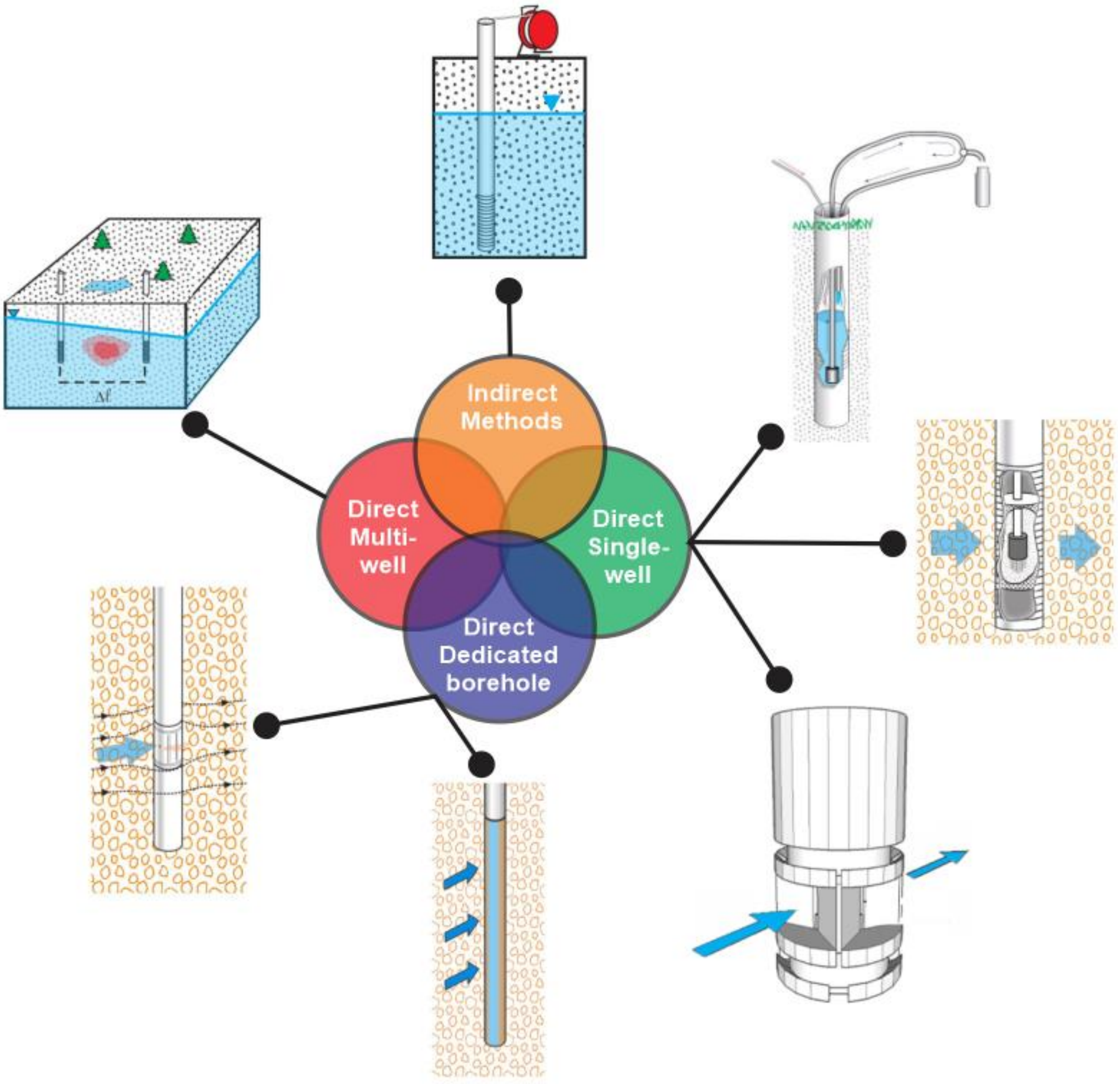

Figure 1 - Contextual diagram showing selected alternative methods for determining groundwater velocity and their general classifications as direct or indirect methods. All are discussed in detail in the following sections of this book. Clockwise from top: Darcy's Law method, point dilution methods, heat pulse flowmeter method, IWPVP, ISPFS, PVP, and multi-well tracer tests.

As contaminants in groundwater have gained attention, and been found to depend — sometimes profoundly — on the details of aquifer structure for their fate and transport behaviors, opportunities to augment Darcy's Law with alternative methods, such as those in Figure 1, have gained attention and value. The efforts to develop these technologies have varied both in approach and level of success. The technologies, discussed in later sections, that have shown promise are summarized in Table 1 and a graphical representation of the areas of strength, by classification from Figure 1, is given in Figure 2.

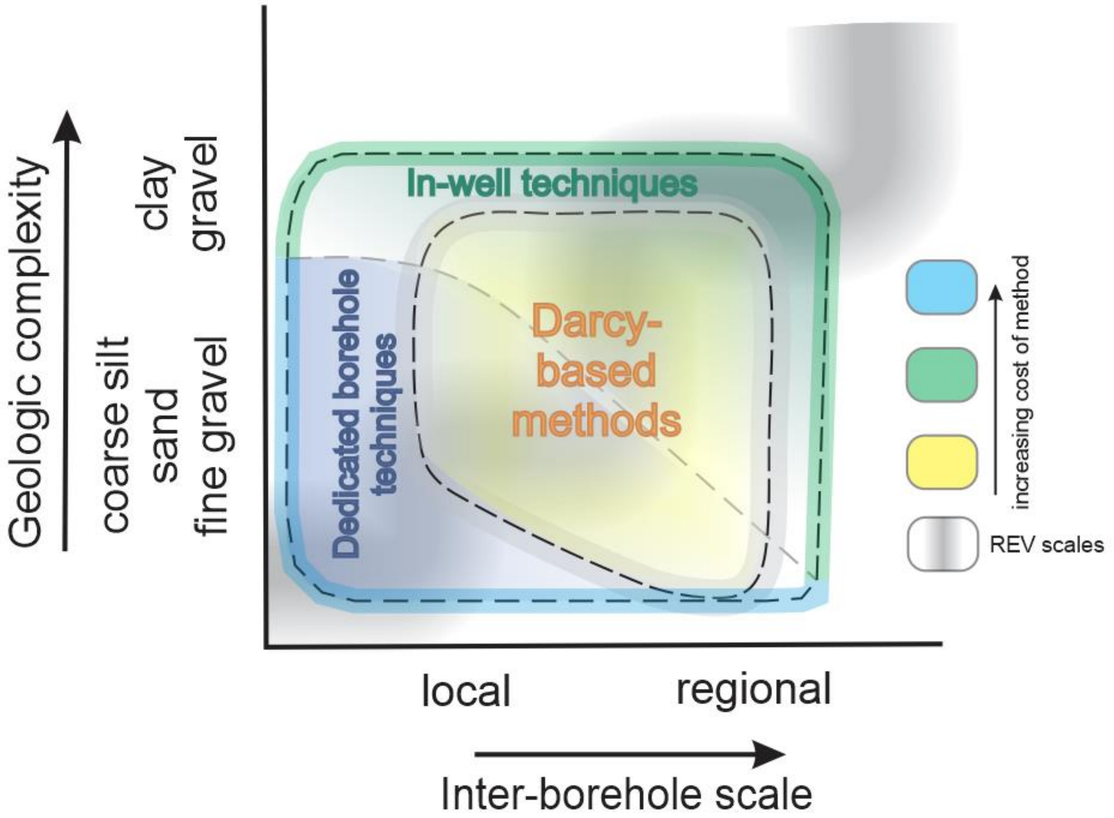

Figure 2 - Conceptualization of the applicability of the groundwater velocity techniques discussed in the text. The vertical axis indicates two aspects: increasing geologic complexity; and sediment texture. The horizontal axis reflects applicability as a function of scale, as defined by borehole spacing. The most reliable results at low scales come from instruments in dedicated holes (no wells) that are not limited by filter packs or well screen interferences. However, the dedicated borehole instruments require complete sediment collapse around the instruments. So, as aquifer sediments become more complex or cohesive, the in-well tools become preferred for small scale measurements. Intermediate scales may be characterized with either single-borehole techniques or Darcy-based methods that are insensitive at lower scales. At large scales (i.e., large distances between wells) Darcy methods suffer from uncertainties in the continuity of geological conditions between wells, so locations needing accurate velocity estimates might benefit from in-well measurements. The gray step pattern in the background of the Figure is a reminder that geologic REVs change with scale.

Table 1 - Summary of groundwater velocity measurement techniques discussed in the text. Within each of the method categories, the range of measurements can extend from a few centimeters per day to tens of meters per day, though this full range of performance is both tool specific and site specific, depending on conditions encountered. Cells colors are matched to Figure 2.

Method	Scale	Examples	Instrumentation/Description	Comments	Application for best advantage
Darcy-based methods	- generally, ~10 m to ~100m separation between wells - local to regional investigations common	- conventional site investigation based on water level survey and estimation of hydraulic conductivity (*K*)	- wells and water level tapes or sondes - measure head in wells for gradient across domain and obtain domain *K* value. Data collection requires minutes per well	- scale dependent on the number and spacing of *K* measurements - scale dependent on the method of *K* measurement - limited by measurable differences in water levels, heterogeneity between wells, and hydraulic connectedness between wells	- generalized flow characterization - forecasting of overall plume migration
		- application of Darcy's Law in digital models	- computer - match field distribution of hydraulic head in a computer model through calibration informed by field data on geology, hydraulic conductivity - generally, requires days to weeks to complete		
In-well velocity techniques	- centimeter to meter scale measurements from single wells - larger scale flow patterns possible with multiple wells and complimentary information (e.g., geophysical, Darcy, modeling)	- point dilution and finite dilution point dilution (FVPD) methods - Drost et al., 1968; Brouyere et al., 2008	- pump, packers, tracer injection system - inject solute tracer into test interval in well and, with mixing, measure concentration decline - requires minutes to hours to complete	- measured flow depends on possible interferences from filter packs (if present), disturbed zone in the borehole outside well casing, and the well screen - best results expected in wells that have been developed extensively - PFM measured time averaged fluxes over days to weeks, other methods return minutes to hours for measurements - Some techniques can be coupled with other sensors or sampling ports	- local flow patterns - verification of Darcy's law calculations - identification of preferred flow zone in vertical profiles - direct velocity measurements in cohesive sediments (silt and clay content), or high gravel fraction
		- passive flux meter (PFM) - Hatfield et al., 2004	- PFM instrument supplied by vendor - deploy instrument into well or borehole and leave for days to weeks - recover instrument and send to laboratory for analysis		
		- in-well point velocity probe (IWPVP) - Osorno et al., 2018	- in-well probe, tracer injection pump, datalogger - deploy in well or borehole, release tracer (saline, deionized water, or heat) - reposition and repeat for profiling - requires minutes to hours to complete each test		
		- colloidal borescope - Kearl and Roemer, 1998	- in-well instrument with camera, up-hole monitor and computer - deploy in well or borehole, allow flow to re-equilibrate, track colloids in water as they pass through the instrument in the well - requires minutes to hours to complete		
		- heat pulse flowmeter (HPF) - Kerfott and Massard, 1985	- probe supplied by vendor must be packed in glass beads and a 'fuzzy packer', up-hole control panel - deploy in well or borehole, activate heater, record temperature changes at thermistors. Interpretation may require expert assistance - requires minutes to complete		
		- direct velocity technique (DVT) - Essouayed et al., 2019)	- in-well device, up-hole tracer injection and detection system - deploy in well or borehole, release tracer into window drain tube at known rate while monitoring outflow concentrations - requires minutes to hours to complete		
Dedicated borehole techniques	- centimeter to meter scale measurements from single boreholes - larger scale flow patterns possible with multiple boreholes and complimentary information (e.g., geophysical, Darcy, modeling)	- point velocity probe (PVP) - Labaky et al., 2007	- probe(s) attached between lengths of casing, tracer injection system and datalogger - deploy instrument as multilevel stack or single in dedicated borehole that is allowed to collapse around the casing - release tracer (e.g., saline, deionized water, heat) and track as it moves on the perimeter of the instrument - requires minutes to hours to complete	- require borehole dedicated to the instrument - subject to interferences related to disturbed zone surrounding borehole - scale depends on number of instruments deployed - PVP can be coupled with other sensors or sampling ports - vertical flow measurable in principle but ISPFS vertical flow data should be interpreted with particular caution	- local flow patterns - non-cohesive sediments (usually high component of sand) - permanent installations suitable for time series measurements - multilevel deployment useful for mass discharge monitoring
		- in-situ passive flow sensor (ISPFS) - Ballard, 1996	- instrument supplied by vendor, up-hole control panel - deploy the instrument in dedicated borehole that is allowed to collapse around the casing - warm the outside surface to steady state and measure final temperature distribution on surface - requires minutes to hours to complete		

Figure 2 is provided only as a general indication of the methods' areas of strength. For example, the greatest strengths of the single borehole methods arise from their ability to identify relatively small-scale geologic features (centimeters to meters in size) that affect contaminant transport in important ways, such as preferred flow channels. Such features can be continuous over large scales, making single borehole methods relevant over any scale of practical value to hydrogeological studies. However, the larger the scale the more measurement points are required to ensure an accurate characterization. This could become cost prohibitive in many cases, so single borehole methods are likely to be most used in investigations at relatively small spatial scales.

Of the single borehole methods, the dedicated instrument methods (probes not expected to be reclaimed from the borehole and reused elsewhere) are expected to be the most reliable because they are subject to fewer sources of bias, such as filter packs and well screens. Offsetting this advantage, is their dependence on good contact between the instrument and the aquifer sediments and this restricts their use to non-cohesive aquifers (with generally high components of sand or fine gravel) and carefully executed methods of emplacement. As geologic complexity increases, an aquifer may be more reliably accessed with a well and the in-well methods may be preferred.

At scales of tens or hundreds of meters, Darcy's Law based approaches are expected to gain utility and cost-effectiveness. As with the single borehole methods, larger scale problems require a larger number of monitoring points, i.e., wells or piezometers, to ensure the variability of the aquifer is represented in the ultimate data set. Nevertheless, in regional scale studies, wells may be placed kilometers apart. Large inter-well spacings tend to reduce the apparent variability in flow, which can be appropriate if a large-scale picture of flow patterns is the goal of the work. If such averaging is of concern — at any scale — then the single borehole methods could provide data that are complimentary to the Darcy-based methods, especially for cases where small and intermediate scales of investigation are of interest.

2 Darcy's Law as a basis for measuring groundwater velocity

Darcy's Law is a disarmingly simple relationship between the rate of groundwater discharge (volume per time) through a specified area of an aquifer ($A = y\ z$ in Figure 3, measured perpendicular to the flow direction) to quantities that can be readily measured, i.e., hydraulic conductivity (K) and the hydraulic gradient (denoted by i, and calculated as the difference in head between two locations, ΔH, divided by the distance between the locations, $\Delta \ell$, $i = \Delta H/\Delta \ell$ in Figure 3). The volume per time, Q, is the product of $K\ i\ A$ or (KiA). Darcy's Law is commonly applied at various scales, with useful insights resulting. However, it should be kept in mind that by utilizing Darcy's Law in this fashion, the hydrogeologist is treating an aquifer as a simple, homogeneous porous medium over the scale being tested. As discussed below, and throughout this book, aquifers are neither simple nor homogeneous, and any measurement made to characterize them will likely vary with the scale of test employed. With this caveat understood, Darcy's Law is worthy of further examination since it has been an underpinning of hydrogeology for over a century and continues to be at the heart of both field and modeling methods for aquifer characterization, resource development, and remediation.

The quantity, *K*, is a measure of the aquifer's ability to conduct water flow and is obtained from any of a variety of field or laboratory tests. Field tests conducted *in situ* are generally considered to produce the most representative values of *K*. The details of these tests can be found elsewhere. For the purposes of this discussion, it is enough to recognize that the values of *K* obtained from any tests can vary spatially, depending on the scale of the test — which can range from the sub-meter scale to tens of meters (Butler and Healy, 1998). Moreover, in aquifers with active chemical or microbiological processes occurring, *K* may also vary locally in time (Schillig et al., 2011). For these reasons, *K* is difficult to pin down in the characterization of an aquifer and is commonly credited as the greatest source of error in Darcy's Law calculations (Bright et al., 2002).

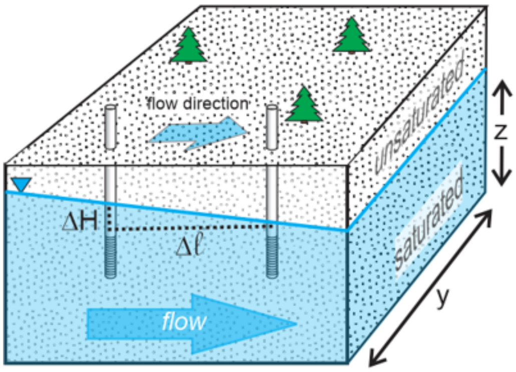

$$Q = -KA\frac{\Delta H}{\Delta \ell} \quad (1) \quad \textit{Total discharge}$$

$$q = -K\frac{\Delta H}{\Delta \ell} \quad (2) \quad \textit{Specific discharge (Darcy flux)}$$

$$v = -\frac{K}{n_e}\frac{\Delta H}{\Delta \ell} \quad (3) \quad \textit{Seepage velocity (average linear velocity)}$$

$Q = total\ discharge\ (L^3T^{-1})$, $q = specific\ discharge\ (LT^{-1})$,

$K = hydraulic\ conductivity\ (LT^{-1})$, $A = cross - sectional\ area\ (L^2)$,

$\ell = distance\ in\ direction\ of\ flow\ (L)$, $H = hydraulic\ head\ (L)$,

$n_e (= effective\ porosity\ dimensionless)$

Figure 3 - Schematic of an aquifer in which groundwater flows from left to right. Darcy's Law (1) relates total discharge through the cross-sectional area, $A = yz$, to the hydraulic conductivity (K) and the hydraulic gradient ($i = \Delta H/\Delta\ell$, which by convention is a negative number in the direction of flow). The negative sign in Darcy's Law is present to cancel the negative sign on the gradient, allowing the quantity Q to be a positive value. Also shown are variations of Darcy's law for the calculation of the Darcy flux, q (also known as the specific discharge) and the seepage velocity, v (also known as the average linear velocity). The value 'n_e' refers to the effective porosity, defined in the text.

The hydraulic gradient, *i*, is generally considered a more reliably measurable quantity than *K*, but it is sometimes also subject to high levels of uncertainty (Devlin and McElwee, 2007). The hydraulic gradient between two locations is obtained by dividing the difference in hydraulic head at the two locations by the distance between them (hydraulic head is expressed as a water level elevation measured from a common datum). Given the accepted practice of ascribing errors in flow calculations primarily to imperfect knowledge of *K*, the issue of error in hydraulic gradient values can be overlooked. Notable errors in *i* may arise from a variety of causes, including a) measurements of water levels in closely spaced wells with nearly identical hydraulic heads, b) measurements in highly permeable sediments, again with small differences in hydraulic head, c) measurements in wells with differing screen lengths that may intersect geologic units in poor hydraulic connection, d) measurements in wells that are not hydraulically connected to each other due to either geological barriers or clogged well screens, e) measurements in wells intersecting zones containing waters of different density (perhaps due to different amounts of dissolved solids), as might occur in deep groundwater systems or near coastlines where seawater intrudes into aquifers (Post and Asmuth, 2013).

The Darcy equation is concerned with the volume of water that passes through a specified area in a given time, i.e., a discharge. It does not make any direct pronouncements on the speed at which the water is moving through that area, only the volume per time. Although at times people speak of a Darcy flux, *q*, which is the product of hydraulic conductivity and gradient (*Ki*) (note: this quantity is also known as the specific discharge because it can also be calculated by dividing the discharge rate by the area through which the water flows) and has units of distance per time, this quantity is not the same as the seepage velocity of a parcel of water as it would be measured in linear distance per time on a map. The distinction might at first seem lost in subtlety. The difference can be easily visualized in the case of water discharging from a common garden hose, held in a horizontal attitude (Figure 4a). If the hose outlet is unobstructed, water will stream out at what might be perceived as a normal rate — the stream moves a horizontal distance of only a few centimeters from the outlet before falling into a 4-liter bucket, for example, which it fills in a minute.

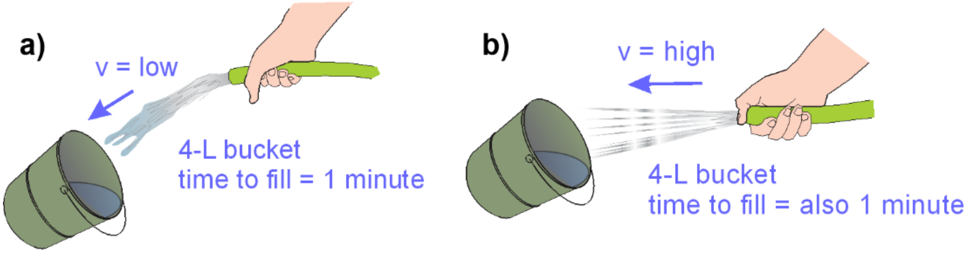

Figure 4 - Water flow from a hose. a) The Darcy flux is the speed (meters per minute) of water flowing from an unobstructed hose. b) The seepage velocity is the speed of water flowing from a hose with an obstructed cross-sectional area. The discharge (liters per minute) is the same in both examples.

Now consider the same hose, with the same four liter per minute flow rate (discharge), but with a thumb partially obstructing the outlet (Figure 4b). The thumb causes the stream of water to exit the hose in a jet of water that may travel horizontally several meters before falling to the ground. The *speed* of the water in these two scenarios is notably different, the first being slower and the second faster, even though it still fills the bucket in a minute. Therefore, the discharge rate is the same in both scenarios. Since the area of the hose perpendicular to flow is unchanging, the specific discharge is also the same in the two scenarios. The Darcy equation is concerned with estimating the discharge or the Darcy flux (specific discharge); the speed can only be obtained if, as in the hose example, the obstruction presented by the thumb i.e., the fraction of the hose area open to flow, is considered.

In this example, the thumb does not reduce the flow rate of water from the hose. The water speed increases because the area available for flow from the hose outlet is diminished. Consequently, pressure builds behind the thumb and drives the resulting water jet. In an aquifer, the obstruction to flow results not from a thumb, but from the solid matrix of the aquifer, generally sediment grains or rock, which contains pores spaces between the grains, analogous to variable diameter tubes. These 'tubes', or pores, are available for water flow, i.e., they are the space not blocked by the thumb in the hose example. The ratio of open space to total space in a volume of aquifer is called porosity, n. For a specified flow rate, the smaller the porosity the higher the backpressure (i.e., up-gradient pressure head) must be to maintain that flow, and the faster water must move through the aquifer. In porous material, some pores are dead ends or not connected to the other pores and do not participate in flow. Only the connected pores that contain flowing water are considered when calculating the seepage velocity. The porosity based on these openings is therefore less than n, and is called the *effective* porosity, n_e. The revised equation for seepage velocity becomes: $v = Ki/n_e = q/n_e$. The direction of the water movement is obtained from the hydraulic gradient term in Darcy's Law; as a first approximation, water flows in the direction given by the steepest descent of hydraulic head.

The above discussion of groundwater velocity is the basis for the majority of field estimates of v and is common hydrogeological practice. As a first pass, low cost, method of aquifer characterization, the method has proven very effective. However, this simplified approach implicitly assumes a homogeneous (K is the same everywhere) and isotropic aquifer (K is the same no matter what direction water moves through the material — essential for the assumption that water flows in the direction of steepest descent of hydraulic head), as well as field measurements that are not subject to scale-related biases. Where significant heterogeneities are present that can channelize flow, or where *in situ* remediation activities require better knowledge of flow behavior on a small scale, greater fidelity than can currently be provided by a field-based Darcy approach may be required. Several specific issues that may demand higher levels of velocity characterization than Darcy's Law calculations typically afford are discussed in the section "The importance of knowing groundwater velocity" later in this book. The search for a reliable alternative — or more likely, reliable complimentary technologies — has produced some promising prospects, and is still underway. Among the issues that must be resolved before such alternatives can gain wide acceptance are 1) reasonably low measurement costs, 2) levels of training to conduct the measurements that do not greatly exceed those currently obtained by college-level hydrogeologists, 3) a measurement scale that makes both theoretical and practical sense, and 4) underpinning all of the above there must be a clear understanding of what the estimated velocity physically represents, otherwise interpretations of the data could be erroneous. This wish list may seem far off presently. However, it continues to drive innovation.

3 Alternative methods for measuring groundwater velocity

Darcy's Law provides a reliable and convenient basis for determining groundwater flow, specific discharge (or Darcy flux) and seepage velocities (hereafter referred to as simply 'velocity' for brevity). However, in response to the complexities discussed above, there are good reasons to develop alternative methods to measure flow, velocity, and flux. To determine groundwater velocities without reference to Darcy's Law is the goal of the so-called *direct* velocity measurement methods. In fact, there are no methods currently available that are capable of *actually* measuring groundwater flow over the entire range of flow rates that might apply. The most versatile and accommodating approaches use tracer detection to *infer* groundwater movement rates. Tracers are substances that dissolve readily in groundwater and that are transported without interferences from chemical or biological processes that might transform them, or temporarily remove them from the water stream (i.e., sorption). Examples include such chemicals as chloride (Cl^-), bromide (Br^-), tritium (^3H), fluorescent dyes, freon compounds (chlorofluorocarbons), and sometimes heated water (e.g. Davis et al., 1980). The techniques vary primarily in 3 specifics: 1) the choice of tracer; 2) the detection method; and 3) the means of access to groundwater i.e., through a well or via direct contact with the aquifer material. Before using a groundwater tracer, it is important to consider the potential impact on groundwater quality and to obtain permission from groundwater oversight agencies, if applicable. The following sections explain the techniques available for various scales of measurement, including inter-well techniques, in-well techniques, and techniques that require direct contact with the aquifer.

3.1 Inter-well tracer tests

Once the tracer approach is chosen to investigate the speed and direction of groundwater flow, additional decisions still need to be made. Among the first is how the tracer will be introduced to the flow system. Depending on the specific questions being asked, tracers might be deployed on the surface, perhaps to examine infiltration or recharge rates, into sinkholes to determine groundwater flow in karst aquifers, or on the bed of lakes and streams to document groundwater-surface water interactions. It is probably safe to say that wells are the most common devices used to investigate flow systems in aquifers in part because they provide readily available conduits for tracer injections. Monitor wells are ubiquitous at sites undergoing hydrogeological investigations since they are used to obtain water level data that support Darcy's Law calculations. A monitor well generally consists of a section of solid casing (a pipe with unperforated walls) and a screen (pipe with perforated or slotted walls). The pieces are assembled and positioned in a borehole with the screened portion on the bottom (Figure 5).

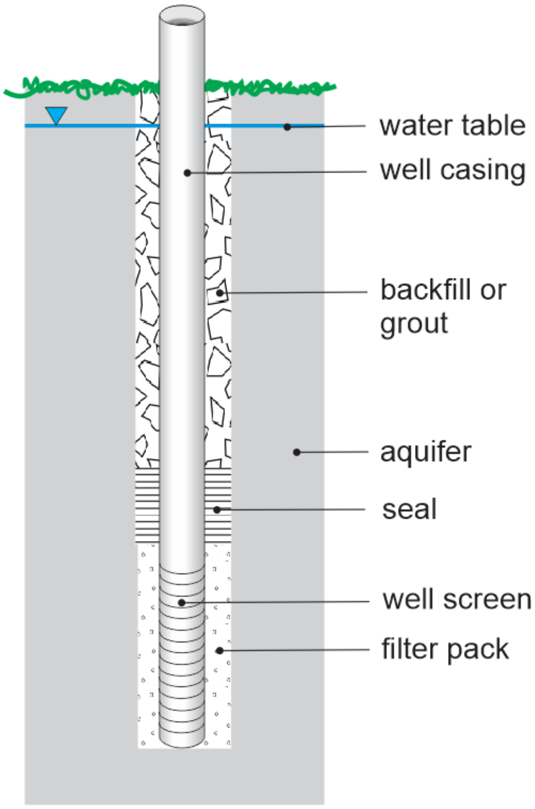

Figure 5 - Schematic of a typical monitoring well (Bedient et al., 1994).

Monitor wells are commonly finished by filling the annulus space (the space between the pipe and the borehole walls) with permeable material around the screen (filter pack), and either backfill material or grout in the borehole above the screen. In some cases, the filter pack is separated from the upper annulus fill material by a seal of bentonite (clay) or cement to prevent contaminants from entering the screened portion of the well through the borehole. Wells can be designed to 'see' specific portions of an aquifer by tailoring the depth of installation and the screen length to the zone of interest. Screens vary in length from less than a meter long to nearly the entire depth of the well. Wells are an integral part of contaminated site investigations and so they are obvious tools for use in tracer studies. Perhaps the simplest experimental design involving tracers and wells is the injection of a tracer into an upstream well, and the monitoring of downstream well(s) for the subsequent appearance of the tracer (e.g., Clement et al., 1997) as shown in Figure 6. Such experiments are called *inter-well tracer tests*, or sometimes *natural gradient tracer tests* when the groundwater flow is allowed to occur under naturally occurring conditions (i.e., without pumping).

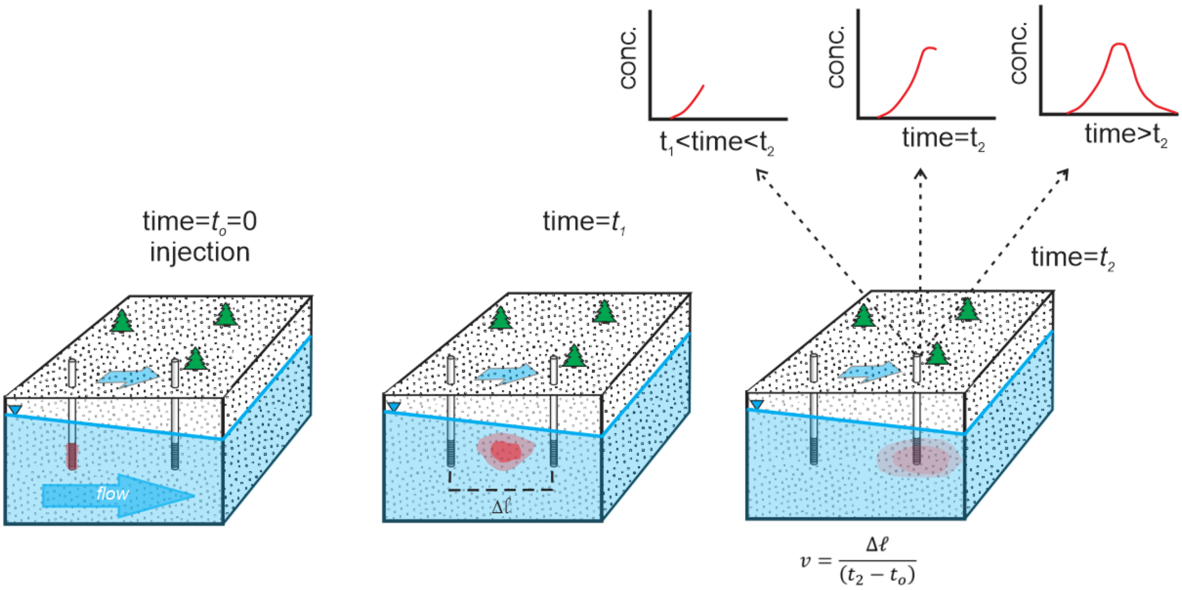

Figure 6 - Idealized conceptualization of an inter-well tracer test. A tracer (red) is injected at time zero, i.e., $t = t_0$, where $t_0 = 0$, and detected at a downstream well at a later time (t_2). If a tracer is introduced as a pulse, the average velocity of the groundwater is found by timing the arrival of the middle of the pulse (i.e., the center of mass, which ideally coincides closely with the highest detected concentration) at the monitoring well. The arrival of the pulse at the downgradient monitoring well begins at a time between t_1 and t_2. The downgradient well may or may not be pumped. The center of mass of the pulse arrives at time t_2. The entire breakthrough history of the pulse is recorded at some time after t_2, as shown in the breakthrough curves above. Ideally, the seepage velocity can be calculated using time t_2 (see equation).

The simplicity of inter-well tracer tests is offset by several problems related to the real-world complexity of aquifers. First, to ensure that the tracer will not be influenced by density driven flow or be entrained by small scale geologic features (strata, lenses), large dilute source volumes in the aquifer must be established; these may not be simple and inexpensive to design or create. Second, more than two wells are likely to be required at close spacings, which makes these tests potentially expensive. Third, if the flow system is not already reasonably well understood, the tracer may be carried along a path that misses even a closely spaced well network — for example by following a path beneath the wells due to unanticipated downward vertical flow, as illustrated for the spill depicted in Figure 7, or by breaking apart into disconnected plumes (Sudicky and Cherry, 1979). Finally, the time required for a tracer to move through the monitor well network may be many days. In extreme cases, many months may be needed for a test to run to completion. Throughout this time, water sampling and analysis is required to properly identify the tracer center of mass or peak arrival time. This requirement can also be expensive to satisfy, although recent *in situ* sensor developments promise to minimize these expenses in the future by automating the tracer monitoring task. Regardless, the time from the onset of a test to its completion may be quite long, delaying decisions that might avert risk.

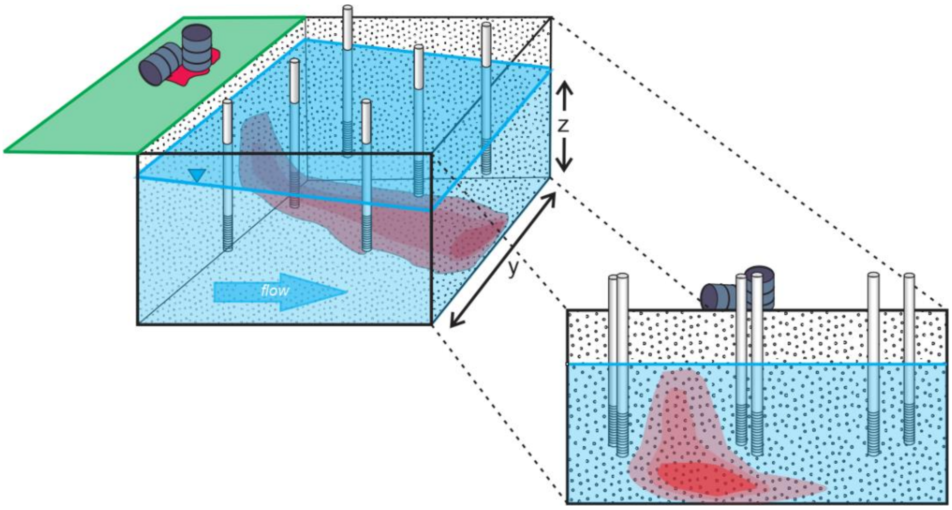

Figure 7 - Illustration showing a multi-well monitor network failing to intersect a plume due to inadequate well spacing and a sinking plume. This scenario could apply to a spill, as illustrated, or tracer tests aimed at characterizing the aquifer — and failing.

3.2 In-well techniques

Tests performed in single wells tend to interrogate a spatial scale much less than inter-well tests, which presents both advantages and difficulties. An advantage of single well tests is that they offer the chance of quantifying the complete range of subsurface flow rates in important locations (Figure 8). Moreover, they are faster and less costly to perform than inter-well tracer tests are likely to be. For this reason, they have received attention over the years. However, the smaller spatial scales they sample — which are not always known with high precision — means that in most cases several tests will be necessary in more than one well location to reasonably define or validate a flow system. Fortunately, if a site is already instrumented with multiple wells, this requirement may not add a great deal of cost to a characterization study.

In keeping with the considerations above, the best known of the direct velocity measurement methods are conducted with equipment deployed in wells, a strategy that has the advantage of convenience but the drawback of a strong possibility of measurement biases caused by the wells, the well screens, and the filter packs. Flow distortions arising from these features can to some extent be estimated in advance and considered during the data analysis stage. However, these calculations assume idealized geometries, fully open well screens, and homogeneous filter packs, which are rarely realized in field applications.

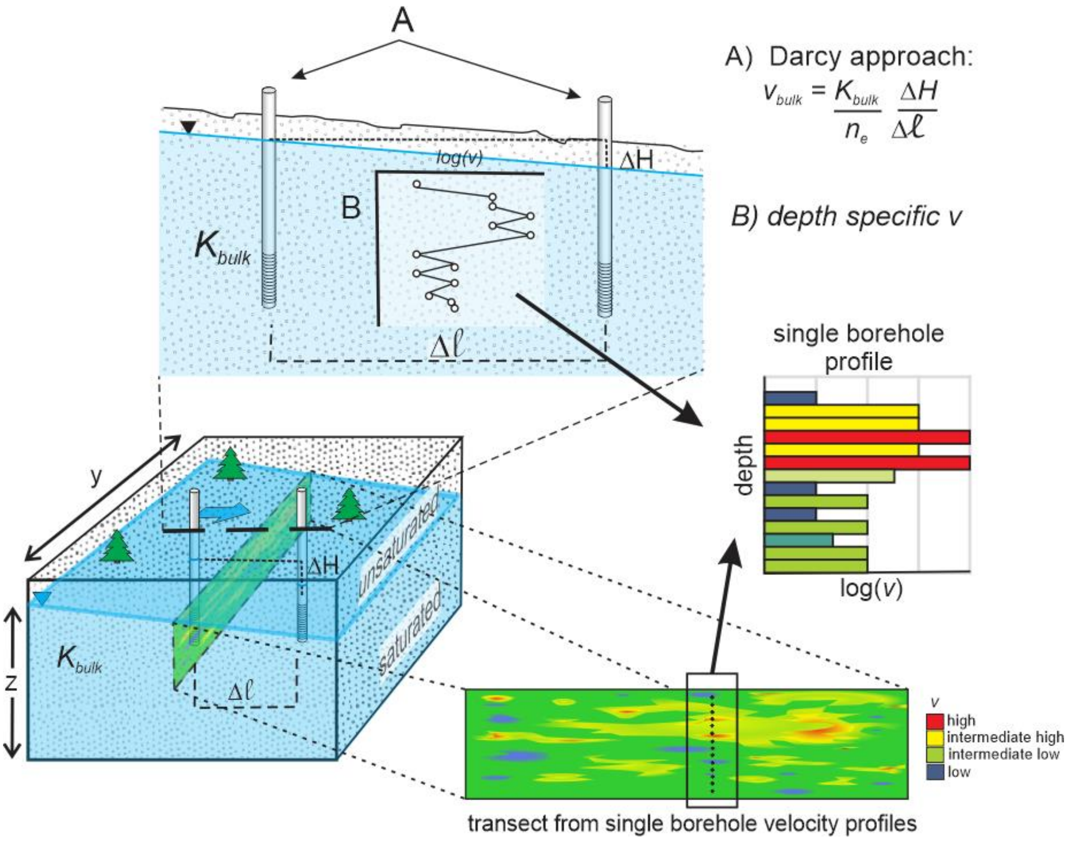

Figure 8 - Comparison of the local velocity information derived from the Darcy calculation and from depth specific velocity measurements. The Darcy approach cannot generally measure small scale hydraulic gradients and therefore produces a velocity value describing the bulk domain. Several single borehole methods are capable of producing vertical profiles of in situ velocity measurements. Previously, this kind of detail was only possible to obtain from grain size analyses or permeameter testing of core materials, and calculations that relied on the ensuing, uncertain estimates of *K*. Profiles like these can be combined from multiple locations to construct transects, as shown above (only one profile shown, for clarity of illustration). Note: in an actual investigation, the *v* presented in the transect would be quantitative, rather than the qualitative descriptors in the legend.

The presence of instruments inside a well, which in some cases may restrict flow through the well, can also invalidate calculations and calibrations that do not include them. Vertical flow in a borehole, or density induced flow, which is manifested more strongly in an open well than in a porous medium, can also create disruptions that confound the accurate sensing of groundwater speed and direction from wells.

Point Dilution Methods

The best known of the in-well groundwater velocity measurement methods is arguably the borehole dilution technique, also known as the point dilution method. A measurement is conducted in a section of a well or borehole that is isolated with packers as shown in Figure 8a, spiked with a tracer, and mixed. The tracer concentration is tracked over time as water flows through the well replacing the tracer solution. The rate of tracer loss is proportional to the ambient groundwater velocity as illustrated in Figure 9 (Drost et al., 1968). A common practice is to use saline tracers (e.g., salts of Cl^- or Br^-) but the effects of solution density on flow from the well can be problematic. A viable response to this problem is to use radioactive isotopes or fluorescent dyes (if permissible by groundwater oversight agencies), since these substances can be introduced and detected at extremely low concentrations — exerting no practical effect on flow related to solution density.

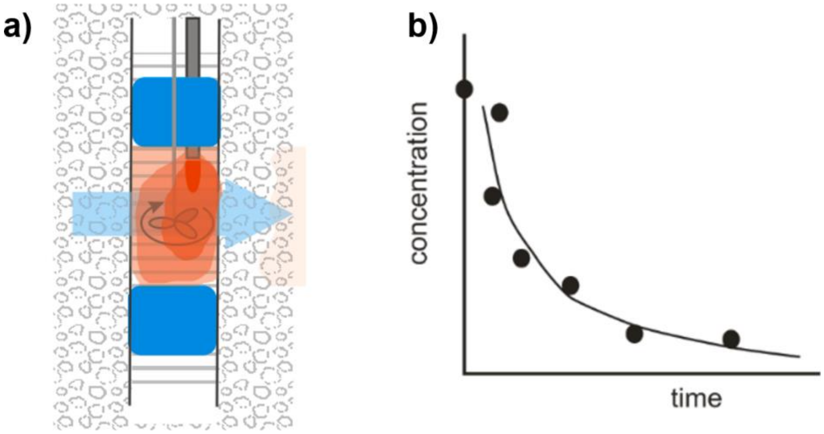

Figure 9 - a) Schematic of the borehole dilution method. Packers (blue) isolate a section of the well while a tracer (red) is mixed (black arrow) with groundwater in the test interval. b) If mixing is continuously maintained, the tracer concentration in the test interval declines exponentially as groundwater passes through the well (see graph).

A variation on the point dilution technique, called the Finite Volume Point Dilution (FVPD) method, involves the continual addition of tracer to the well while water is recirculated to achieve mixing in the well as shown in Figure 10 (Brouyere et al., 2008).

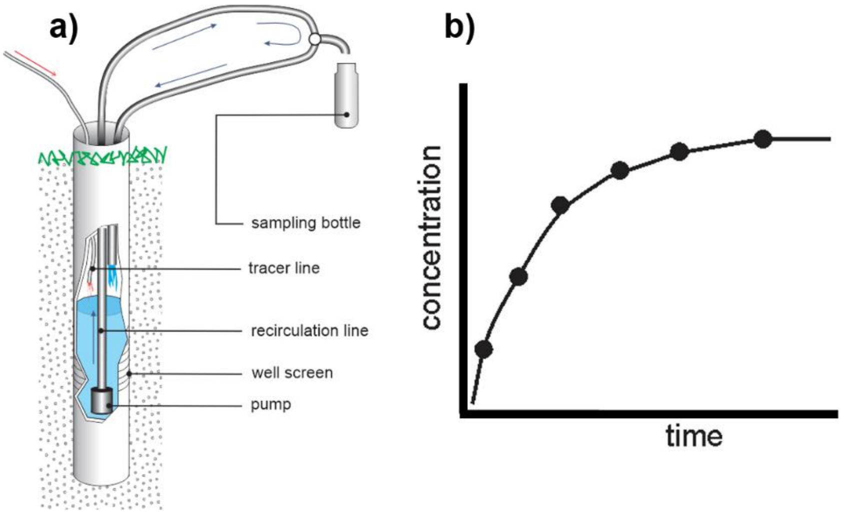

Figure 10 - a) Schematic of the finite volume point dilution technique. b) If mixing and tracer injection are continuous, the tracer concentration rises to a plateau over time.

The steady state concentration of tracer that develops in the well is a function of the flow rate entering the well from the aquifer, provided the tracer injection rate is low compared to the groundwater flow rate through the well. If the tracer concentration in the well at the beginning of an FVPD test is zero, then the tracer concentration rises in the well over time to a final plateau value. The flow rate can be calculated from either the rising portion of the curve, the plateau, or both. Similarly, an analysis can be performed to determine groundwater flow rates based on the falling curve of a subsequent well flushing test.

Heat Pulse Flowmeter

A tracer that offers several advantages for groundwater velocity measurements is heat. Heat is easy to introduce to the subsurface and can be detected, through temperature measurements, with great precision and accuracy. Unfortunately, heat also brings with it some serious challenges. For example, the density of a solution is sensitive to its temperature, so measured flow rates can be biased by heating groundwater. In addition, heat transports in both solids (diffusively) and water (advectively and diffusively). The rate of transport in the solids depends on the thermal conductivities of the solids. These coefficients are generally assumed to be uniform and constant in the well and formation, which may introduce errors in some cases. An instrument that uses heat to measure groundwater velocity was introduced in the mid-1980s and is commonly referred to as the Heat Pulse Flowmeter (HPF), or Geoflometer® (Kerfoot and Massard, 1985). The device works by heating water in the center of the device, typically deployed in the screened portion of a well, and then allowing flow to carry the warmed water past an encircling array of thermistors. The rate that groundwater moves through the system is calculated from the arrival time of the tracer at the detectors, and the flow direction is determined on the basis of which detectors respond (Figure 11).

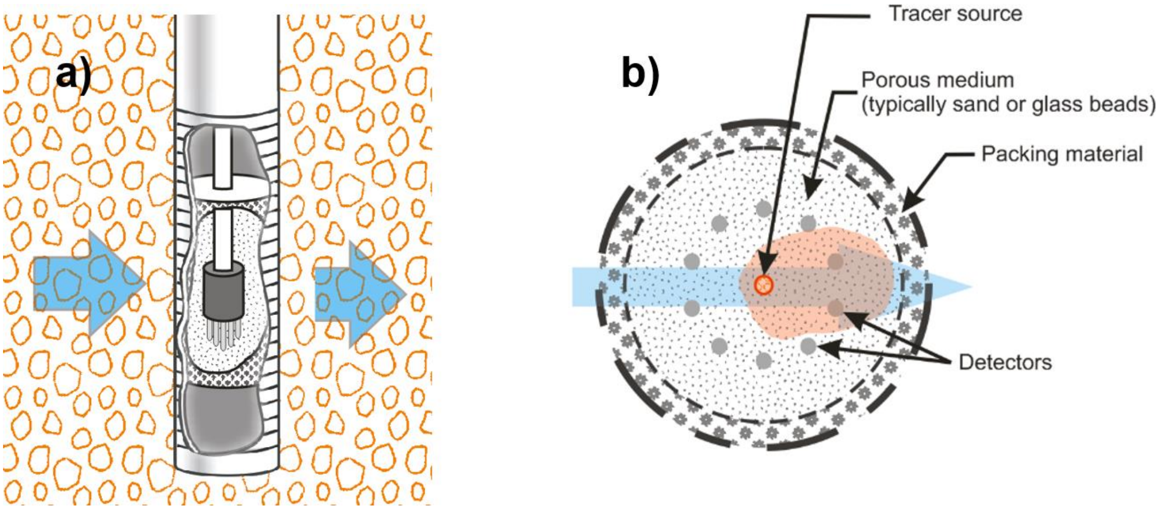

Figure 11 - Schematics of the heat pulse flowmeter. a) Depiction of the instrument packed inside a porous medium within the well. The housing containing the probe is jacketed with a porous material that seals the annular space between the inside of the screen and the probe housing. b) Plan view of the spatial relationships between the tracer release point (center) and the surrounding detectors. Flow is indicated by blue arrows. The tracer pulse is indicated in shades of red.

The HPF was an early technology for direct measurement of velocity at small scales (~10 cm) and this may, in part, account for a mixed record of success. Practitioners accustomed to flow systems defined by water level surveys might understandably question the validity of a method that detects high levels of variability that are invisible to the Darcy approach of estimating velocity. Indeed, instrument limitations may have been the source of some of these errors. For example, flow directions have been sometimes found to be self-contradictory (i.e., thermistor responses both upstream and downstream simultaneously in the same well) with these probes, for reasons that are not understood.

In Well Point Velocity Probe

Another device that functions by tracking a tracer released in the center of a flow-through probe is the In Well Point Velocity Probe (IWPVP) as shown in Figure 12a (Osorno et al., 2018).

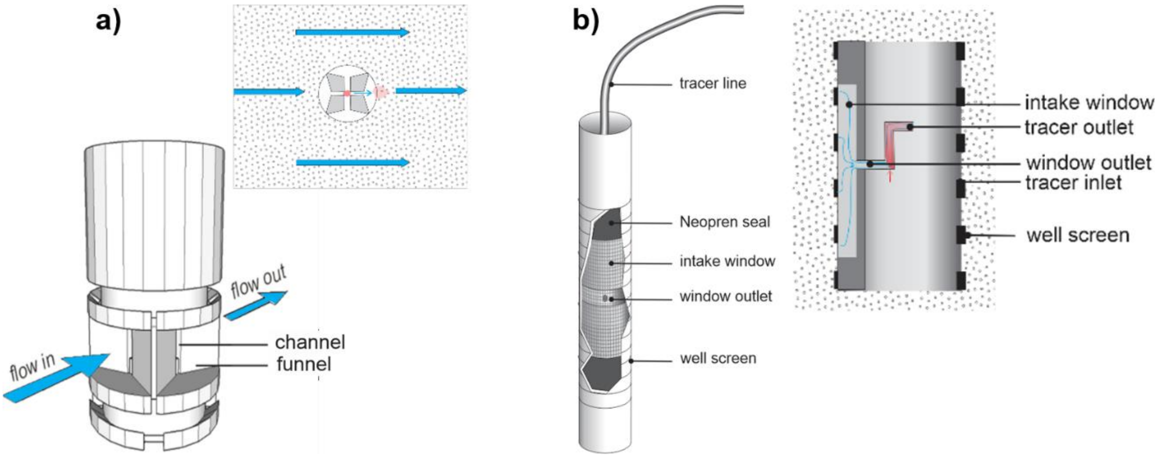

Figure 12 - a) The In-Well Point Velocity Probe. This device is placed in the screened portion of a well where water entering the well is directed through one or two upstream channels. Water leaves the probe through the downstream channels where a tracer, introduced in the center of the probe, is detected. Inset shows a horizontal cross-section to illustrate tracer path from the center of the probe (the release point) through an exit channel, to the aquifer. b) The Direct Velocity Tool. Water is collected in the window and exits through the outlet tube. Tracer is added to the water stream in the tube and is diluted by the stream. The diluted tracer is detected as water leaves the tube. Inset shows a vertical cross-section that illustrates the path of the water entering the collecting window and its direction through the tracer introduction tube.

This instrument differs from the HPF by restricting the flow path out of the probe to four channels with detectors. This restriction simplifies data interpretation by reducing the number of detection signals that must be analyzed. The device makes single measurements of velocity at the centimeter scale but can be repositioned in a well-screen to obtain profiles of velocity with depth. It can also be fabricated in a multilevel fashion that can reduce the number of times repositioning is necessary to obtain velocity profiles. The device currently relies on tracers detected with electrical conductivity detectors, but the design could also support heat or other tracers.

Direct Velocity Tool

The Direct Velocity Tool (DVT) also operates on the principle of capturing groundwater with a well, directing it through an instrument where a tracer is added and then detected as it leaves the device as shown in Figure 12b (Essouayed et al., 2019). The DVT also uses saline tracers, which it detects with electrical conductivity sensors. However, the design differs from the IWPVP in two major ways: first, water is collected from a single, fixed portion of the well screen — requiring advanced knowledge of the flow direction, or repositioning of the device in the well to find the flow direction — and second, the tracer is added continuously to the groundwater stream during testing; the IWPVP introduces the tracer as a low volume pulse. The DVT estimates velocity from the degree of tracer dilution in the groundwater stream rather than timing the arrival of a tracer pulse.

Passive Flux Meter

Other in-well devices for measuring groundwater velocity include the Passive Flux Meter (PFM), which measures water or solute fluxes by quantifying the elution (i.e., dissolution and transport out of the instrument) or collection of tracers and contaminants on sorptive materials placed in a well (Hatfield et al., 2004). The PFM method returns Darcy flux values rather than seepage velocities, making it complimentary to other direct velocity measurement methods. The PFM has been adapted for various hydrologic settings, including fractured rock wells, hyporheic zone settings, and groundwater-surface water interfaces.

Colloidal borescope

The colloidal borescope is a down-well instrument that comprises a light source and a camera mounted about 0.25 m apart. The light illuminates colloidal solids suspended in groundwater passing through the well, and the camera records the movement. Software tracks the individual colloidal particles and the statistical distribution of colloid velocities in the well is then determined (Kearl and Roemer, 1998). The predominant colloid velocity is taken as indicative of the seepage velocity outside the well through correction factors. In principle, the instrument is useful for velocities in the low centimeters per day range to several meters per day. However, in some cases, particularly those involving low flow environments, the colloid movement in the well has been observed not to settle on a clear, predominant, velocity. Therefore, the technology may gain effectiveness as seepage velocities tend to the higher values characteristic of groundwater.

3.3 Techniques involving direct contact with aquifer material

To avoid the problems associated with wells, filter packs, and well screens, techniques that allow sensors to be in direct contact with an aquifer matrix were developed. Two of the direct-contact *in situ* probe types that have received attention on the strength of their performances in field tests are the In Situ Permeable Flow Sensor (ISPFS), later renamed Hydrotechnics™ groundwater velocity sensors, and the point velocity probe (PVP) as shown in Figure 13a and b.

In Situ Permeable Flow Sensor

The ISPFS consists of a nearly one-meter long cylinder with a surface that is uniformly heated and monitored for temperature with a dense network of sensors as shown in Figure 13a (Ballard, 1996). The instrument is installed in dedicated boreholes established in unconsolidated, non-cohesive porous media. The disturbed sediments collapse against the probe leaving no open channels for flow in the borehole annulus. Groundwater flows up to and against the probe, cooling the upgradient side compared to the downgradient side. Patterns of temperature on the overall surface are then related mathematically to groundwater velocity (i.e., speed and direction). In practice, the sophistication and associated cost of the instrument restricts its use to large, well-funded projects. The length of the probe limits its ability to discern fine hydrogeologic and plume features, and is best suited for use in relatively thick, homogeneous aquifers or strata. Since the probe uses heat as a tracer, it is sensitive to density-induced flow and variations in thermal conductivity in the surrounding formation. The technology has been associated with spurious detections of vertical flow — particularly when installed with a filter pack or when installed across sediment interfaces with different thermal conductivities (Ballard et al., 1996; Su et al., 2006).

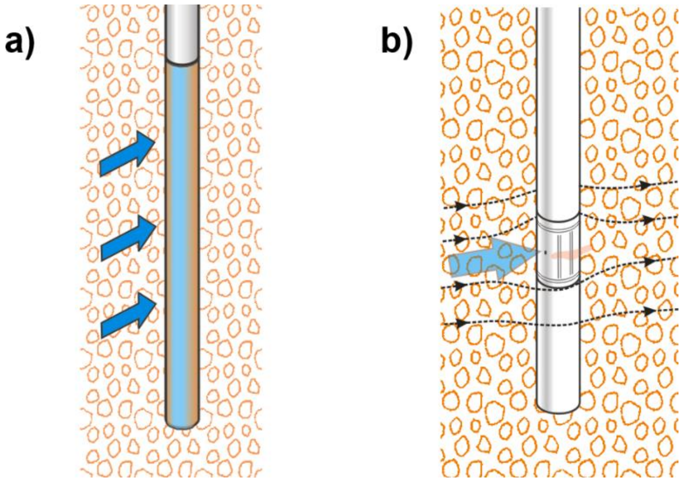

Figure 13 - Schematic diagrams of the a) ISPFS and b) PVP

Point Velocity Probe (PVP)

The PVP, like the ISPFS, is a cylindrical probe installed in a dedicated borehole. However, the PVP senses water movement by recording the breakthrough curve of a tracer rather than a temperature distribution. In principle, the PVP tracer could be a radioisotope, a dye, heat, a conductive solution, or even deionized water — anything that could be detected *in situ* with a small sensor (Labaky et al., 2007). To date, the tracer most commonly used has been a dilute (<1 g/L) saline solution, which provides an electrical conductivity signal well above background in freshwater. The probe operates by releasing a small volume (<1 mL) of the tracer, which is carried by groundwater over the probe's surface to conductivity detectors (Figure 13b). With at least two such detectors on the probe, both speed and direction of the horizontal water movement can be calculated at the centimeter scale. If detectors are placed above and below the tracer release point, vertical flow can also be quantified (Gibson and Devlin, 2018). The probe can be mounted in a multilevel arrangement, permitting as many as 7 probes to instrument a single borehole. The probes have performed well in both sandy, and glacial outwash aquifers. In deposits with elevated clay content, the collapse of the borehole against the probe body tends to be incomplete and reliable data cannot be collected.

Groundwater Variability Probe

A variation on the heat pulse flowmeter design, for use in near surface (<1 m depth), dedicated, uncased boreholes is the Groundwater Variability Probe (GVP) (Crawford et al., 2016). This device is installed in direct contact with aquifer material, and like the HPF is fabricated with several sensors arranged in a ring around a central tracer release point. In principle, data interpretation is simple and based on the time of arrival of the tracer at the sensors, with the affected sensors indicating the flow direction. However, the device is susceptible to biases if the sediment between the sensors is disturbed during installation.

4 The importance of knowing groundwater velocity

The spread of dissolved pollutants from a source area by groundwater movement typically produces a contaminated zone referred to as a plume. The greater the groundwater velocity, the faster the plume grows. Plumes may be generated in many different shapes and sizes, but they share the common attribute of growing primarily in the net downstream direction of groundwater flow. In flow systems with a single predominant flow direction, and an aquifer comprising sediments lacking geologic complexity, such as preferred or channelized flow, plumes will develop into long, thin zones, resembling a sausage shape. It is interesting to note that this notion of plumes is contrary to earlier thinking, where, in the 1980's, it was common to see conceptual models assuming substantial lateral spreading of dissolved solutes due to transverse (horizontal or lateral) dispersion. Since then, high resolution groundwater sampling and tracer studies have led to the 'weak dispersion' view of plumes. Site characterization efforts are commonly designed to identify the boundaries of a plume. However, the number of monitor wells (hence expense) required to outline the shape of a long, thin plume with sufficient fidelity to confidently document plume growth or attenuation can be impractical.

To overcome this difficulty, attempts may be made to instrument the plume along its centerline as shown in Figure 14 (McNab and Dooher, 1998). Finding a plume centerline is not straightforward. A possible approach is to first characterize the plume with high-resolution depth-discrete groundwater sampling using one-time sample collection devices (e.g., hydropunch™ methods or Waterloo APS™ Vertical Aquifer Profiling Technology, and others). By aligning closely spaced depth-discrete sampling locations aligned in transects perpendicular to the plume axis, the plume can be characterized in three dimensions, and the location of the centerline defined with reasonable accuracy. The advantage of this approach is that, with relatively few monitoring wells, data can be gathered that establish the greatest extent of the plume in the predominant direction of growth, and the resulting profile of concentrations can be used to infer plume spreading rates and attenuation rates. The advantage of this approach is also its weakness; the use of few wells translates to low confidence that the actual centerline is being monitored with clear implications for the reliability of the subsequent interpretations.

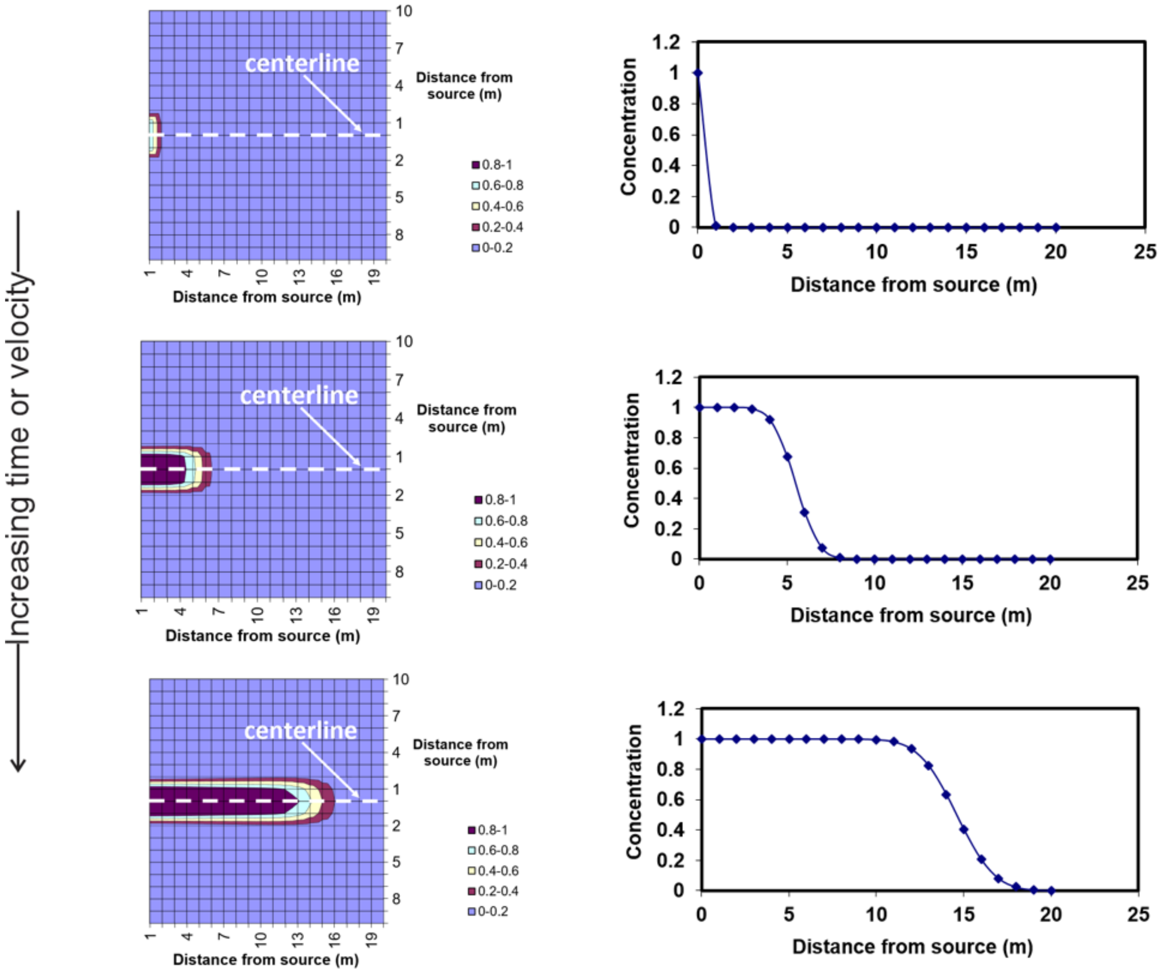

Figure 14 - The growth of a simple plume of groundwater contamination as seen in plan-view with groundwater flow from left to right. The x-axis refers to distance from the source in the direction of flow (longitudinal), and the y-axis refers the distance from the source perpendicular to flow (transverse). In the absence of geological complexities, or pronounced variations in flow over time, plumes will grow into thin, straight zones. Instrumentation along plume centerlines can provide information detailed enough to document plume growth or attenuation in time. In the simulations undertaken to create these images, *v* was set to 0.04, 0.15 and 0.4 m/d, the longitudinal dispersivity was set to 0.1 m. Horizontal transverse dispersivity was set at 0.01 m and vertical transverse dispersivity was set at 0.0015 m.

With the above conceptualization of plumes in mind, the average hydrogeologist would likely advocate the use of groundwater velocity measurements first and foremost to predict the earliest arrival times of contaminants at various receptors (e.g., water wells and surface water bodies). In today’s climate of risk-driven corrective action for groundwater contamination, that objective is very reasonable but incomplete. Since real-world plumes exhibit more complexity than the simple case shown in Figure 14, the case can be made that without a proper — i.e., more detailed — understanding of groundwater velocity, or flux, at a site (note that Darcy flux measurements provide the same essential information for the examples presented below and may be substituted for seepage velocity in many situations), very little else can be known with much certainty.

To illustrate the fundamental importance of velocity, consider the following characteristics of contaminants and aquifers that are commonly estimated without a detailed consideration of groundwater velocity: transformation rate constants (parameters from which the apparent rates of chemical reactions can be calculated), oxidation or reduction capacity (the capacity of the dissolved chemicals to gain or lose an electron to one another or to aquifer solids), groundwater mixing, residence times, and contaminant mass flux across a boundary.

4.1 Rate Constants

Transformation rate constants are essential for the assessment of natural attenuation (an aquifer's ability to reduce a plume of contamination without human intervention) as a strategy for site reclamation. For example, in some jurisdictions, the Risk Based Corrective Action (RBCA) approach is used for defining the level to which humans need to remediate a subsurface source of contamination depends on the natural attenuation factor (NAF), which is estimated as the ratio of the source concentration to the concentration reaching a receptor, at steady state (Begley, 1996). The NAF represents natural attenuation processes, usually biodegradation or abiotic degradation, and combined with the maximum concentration limit (MCL) permitted at the receptor, is used to back-calculate the maximum contaminant levels permissible at the source. Tabulated values of rate constants are available to assist with the parameterization of models, and where these values are unavailable or where concern exists that the available values may not be representative, laboratory tests may be undertaken to obtain them. However, neither of these data sources represents the site-specific dynamics of flow in the ground — they are concerned only with the chemical transformation rates, and some values may assume perfectly mixed solutions. As a result, no matter how accurate they are, they are incapable of anticipating the size of a contaminated zone resulting from the transport of pollutants by groundwater, i.e., the plume size, without accurate knowledge of the flow system, in particular the seepage velocity or Darcy flux. This concept is easily demonstrated by comparing two plumes of trichloroethane (TCA), which transforms to 1,2 dichloroethene and acetic acid through an abiotic reaction with water, with a well-documented half-life ($t½$) of about 2.3 years (assuming T ≅ 15 °C) as shown in Figure 15 (note: a half-life is the time required for the pollutant concentration to decrease to half its original value).

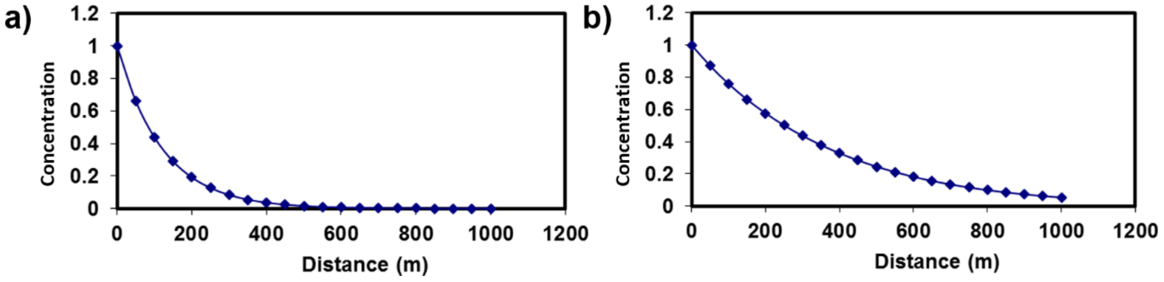

Figure 15 - a) Steady-state plume centerline profile of 1,1 trichloroethane in an aquifer with v = 10 cm/day and $t½$ of 2.3 years. Plume size is sufficiently wide and deep that the boundaries do not influence the concentrations on the centerline. b) The same plume steady-state centerline profile with v = 30 cm/day. Prior knowledge of the rate constant (through $t½$) is not deterministic of the plume size without good knowledge of the groundwater velocity. (In these calculations, longitudinal dispersivity was fixed at 0.1 m, horizontal transverse dispersivity was set to 0.01 m, and vertical dispersivity was set to 0.015 m.)

If such a plume is permitted to grow to its steady-state length, and a groundwater velocity of 10 cm/day is assumed to apply, the plume front (taken here to be C/C_o = 0.01, for convenience, where C is the pollutant concentration at a specific place and time and C_o is the pollutant concentration at the source) will reach a distance of about 550 m from the source. If the groundwater velocity is taken to be 30 cm/day — within the range of uncertainty typically afforded by seepage velocity estimated from Darcy calculations, which rely on hydraulic conductivity — the plume length will reach about 1500 m. This difference has profound implications for the risk experienced by receptors downgradient of the source area, and this is a case in which the transformation rate is highly reliable and predictable. In this case there appears to be a simple proportionality to the problem: tripling the seepage velocity tripled the length of the plume. This simplicity is, unfortunately, not generally assured.

A common scenario involving variable transformation rates involves the biodegradation of petroleum hydrocarbons in the presence of dissolved oxygen, or other so-called terminal electron acceptors (TEA). In these reactions, the hydrocarbons give up electrons to the TEAs as carbon leaves the hydrocarbon molecules and becomes carbon dioxide. The reaction rates in this case are limited by availability of the TEAs, and if TEAs are present the reactions can be regarded as instantaneous (Rifai and Bedient, 1990). TEA availability turns out to be dependent on the degree of mixing in the subsurface (this issue is discussed in more detail in the section "Subsurface Mixing" later in this book), which brings the dissolved hydrocarbons and TEAs into contact. Thus, the transformation rate depends on transport processes. Once the supply of TEA is exhausted, the transformation of hydrocarbons stops. The resulting non-proportional relationship between plume length and seepage velocity is illustrated with a simple calculation of such a biodegradation scenario (Figure 16). In this case, increasing the seepage velocity from 10 cm/day to 30 cm/day only advances the plume front from about 190 m to 255 m from the source. Other biodegradation rates, which depend on particular geochemical environments for transformation to occur, are affected — sometimes completely disrupted — in still more complex ways by the inflow of interfering chemicals (e.g., dissolved oxygen flowing into a zone of reductive dechlorination) and can be highly sensitive to groundwater velocity.

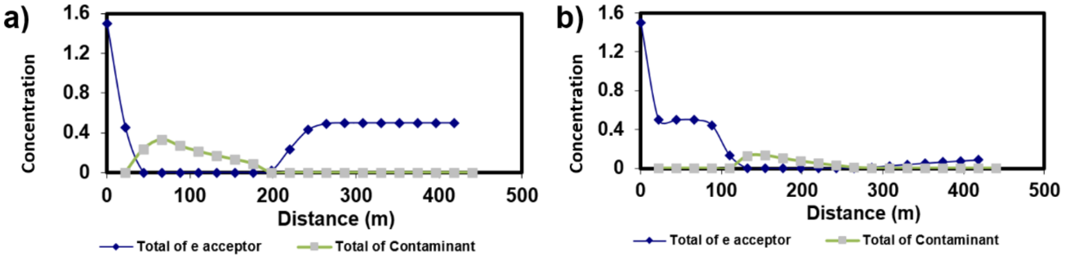

Figure 16 - Two cases of a contaminant reacting with an electron acceptor in a flow system. In both cases the electron acceptor is present in the background water at a concentration of 0.5 M/L^3 and has been injected at the source at 1 M/L^3 for one year. The plumes are modeled in three dimensions. The contaminant is introduced at 1 M/L^3 and has been released for 15 years. a) Plume center line profiles for an oxidizable contaminant and an electron acceptor in an aquifer with a *v* of 0.1 m/day. b) The same plume center line with a *v* of 0.3 m/day. Reactions between the contaminant and the electron acceptor are assumed to be instantaneous. The electron acceptor was assumed to move in the aquifer without retardation, and the contaminant was assumed to migrate with a retardation factor of 2.5, typical of simple hydrocarbons.

4.2 Oxidation-reduction capacities

Natural attenuation sometimes relies on the capacity of an aquifer matrix to supply electrons (reduction of pollutant) or consume them (oxidation of pollutant) to drive pollutant transformations and attenuation (Barcelona and Holm, 1991). In the case of reduction capacities, examples of electron sources include natural organic material (NOM), or reduced elements in minerals making up the aquifer matrix. Examples of pollutants that can be abated by reduction reactions include nitrate (to dinitrogen gas) via denitrification, chromium via a conversion from the mobile Cr^{6+} state to the immobile Cr^{3+} state, or the dechlorination of solvent compounds such as trichloroethene. Prior to the introduction of a pollutant, an aquifer may be near geochemical equilibrium, with the reduction capacity essentially stable and at steady state. The introduction of the pollutant begins a progressive consumption of the reduction capacity, from the source area to regions down-flow, as the pollutant contacts the matrix material (Figure 17).

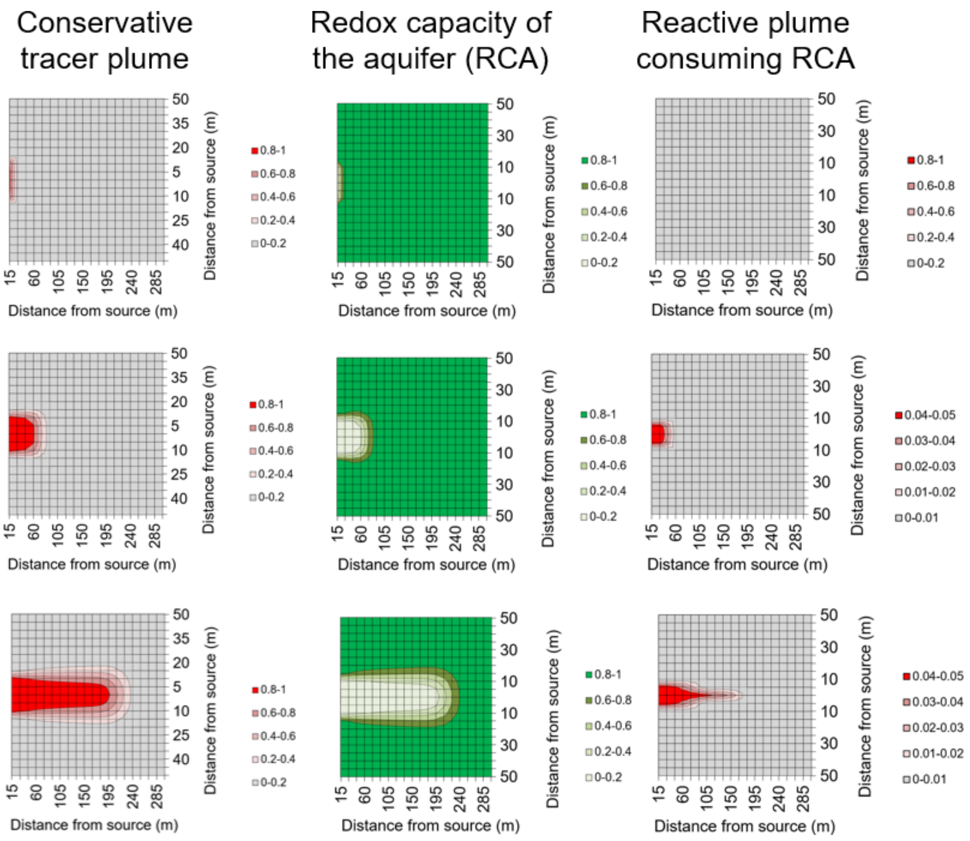

Figure 17 - Progression of contaminant plumes (in plan-view with time advancing down the table) behaving conservatively (left) and susceptible to transformation by oxidation or reduction in an aquifer with a redox capacity (right). The plume growth is retarded by the mass loss due to reaction, and the aquifer redox capacity consumed progressively from left to right over time (center).

The same reasoning applies to aerobic aquifers except that an *oxidation* capacity is established in the matrix and is progressively exhausted by pollutants initially in a reduced state (e.g., petroleum hydrocarbons).

The velocity of the groundwater is highly determinative of the time that the aquifer will maintain its capacity to attenuate a pollutant. This relationship follows from simple mass balance considerations. The problem, in a highly simplified form, can be understood with the following analogy: an unending stream of hungry children moves down a grocery store aisle stacked with cookies. The children eat the cookies as they encounter them, first at the aisle entrance and then progressively deeper into aisle over time. The store owner can quickly appreciate that his inventory will be depleted sooner if the children run down the aisle rather than walk.

Real-world aquifers are to some degree heterogeneous and are therefore unlikely to lose their redox capacity in the purely progressive way described above. Pathways of faster flow will interlace with pathways of slower flow leading to a comparatively complex distribution of redox capacity changes in most cases. This could lead to earlier breakthroughs of pollutants than might otherwise be expected. Predicting the timing of these breakthroughs in some heterogeneous materials, requires detailed characterization of flow patterns, at the centimeter to meter scale.

4.3 Subsurface mixing

For the purposes of this discussion, the term (groundwater) 'mixing' will refer to the blending of solutions in the subsurface at the molecular scale, i.e., a scale at which mass transfer limitations imposed on chemical reaction rates, even between neighboring pores, can be completely discounted. Historically, the mixing of pollutants and ambient groundwater has been ascribed to a process that hydrogeologists refer to as 'hydrodynamic dispersion', or sometimes simply 'dispersion'. In the absence of dispersion, plumes are transported by the advective process alone, referred to as *plug flow* (Figure 18), and no mixing with the background water occurs. So, dispersion might simply be regarded as the combination of transport processes that causes plume to depart from plug flow behavior (Anderson, 1984).

Typically, dispersion is quantified in models based on a differential equation called the advection-dispersion equation. Unfortunately, the mixing represented by dispersion in this equation is geared at describing plume shape and extent empirically — as determined by the monitoring network in use — and is not necessarily indicative of *mixing in the aquifer at the molecular scale*. Confusion over this subtlety has implications for activities that depend on mixing. For example, mixing should increase the volume of an aquifer affected by a pollutant, making plumes easier to locate and delineate for remediation purposes. Complete molecular scale mixing in an aquifer is not an absolute requirement for this outcome, as long as monitoring wells can intercept detectable concentrations of the contaminant. The same may be true for the assessment of first arrival times of pollutants at receptors. Increased mixing — even mixing that is not complete at the molecular scale — leads to a plume front that extends beyond the plug flow front, resulting in pollutants that arrive sooner than predicted by average velocities, i.e., sooner than expected, at receptors (Figure 18). Molecular scale mixing will result in the *dilution* of dissolved substances, i.e., the uniform lowering of concentrations (mass per unit volume) due solely to replacement of solute mass by water mass in a given volume. Note that mixing at scales larger than the molecular scale may give the appearance of dilution in samples but may actually leave some zones in the subsurface unmixed and others solute-free — the blending of these zones occurs in the well or during sample collection. Therefore, molecular scale mixing is necessary for the dilution of pollutants, which in cases of chemicals that pose low risk to health or ecosystems might mean that humans need not actively respond to the release. Furthermore, as mentioned in the previous section, pollutant degradation by natural attenuation, or via engineered systems, may depend on the presence of dissolved electron acceptors (e.g., dissolved oxygen, nitrate or sulphate), or other reaction-enhancing solutions that humans inject into the subsurface to ameliorate a contamination problem. To be effective, these substances must mix with the polluted water volume at the molecular scale; high rates of mixing lead to the highest degradation rates the chemistry allows. Finally, contaminant plumes do not grow in length indefinitely. The maximum length a plume will grow is determined by contaminant mass loss rates due to radioactive decay or transformations — affected by mixing, as discussed above — and dilution achieved by dispersive mixing (particularly along the plume margins) at molecular scales. Mixing by dispersion depends on variability in both groundwater velocity (Figure 19) and contaminant (or other solute) concentration (Figure 20) (Cherry, 1990).

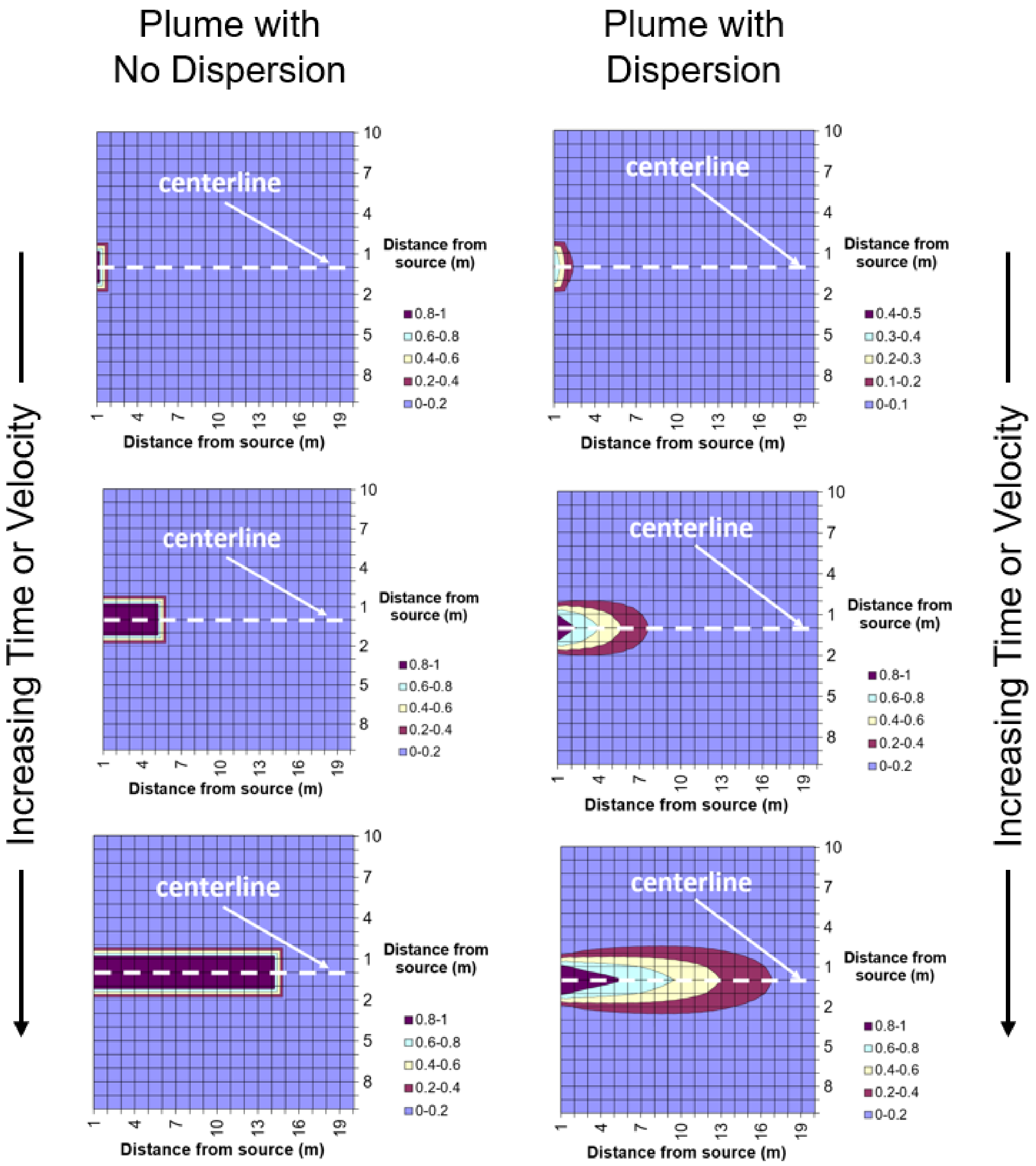

Figure 18 - Plan view of the growth of a simple plume of groundwater contamination with and without the process of dispersion. The plume growing without dispersion illustrates 'plug flow' and is purely advective transport. The plume growing with dispersion illustrates the diluting effects dispersion imposes on a plume, as well as extending the volume of aquifer that is contaminated. In the longitudinal direction (the direction of flow), this extension results in slightly earlier arrival times of the pollutant at receptors. These simulations were performed with the same transport parameters as those given in Figure 14 except that the 'no dispersion' calculations used dispersivities < 0.001 m, and the 'dispersion' calculations used a longitudinal dispersivity of 1 m, a horizontal transverse dispersivity of 0.1 m and a vertical transverse dispersivity of 0.015 m.

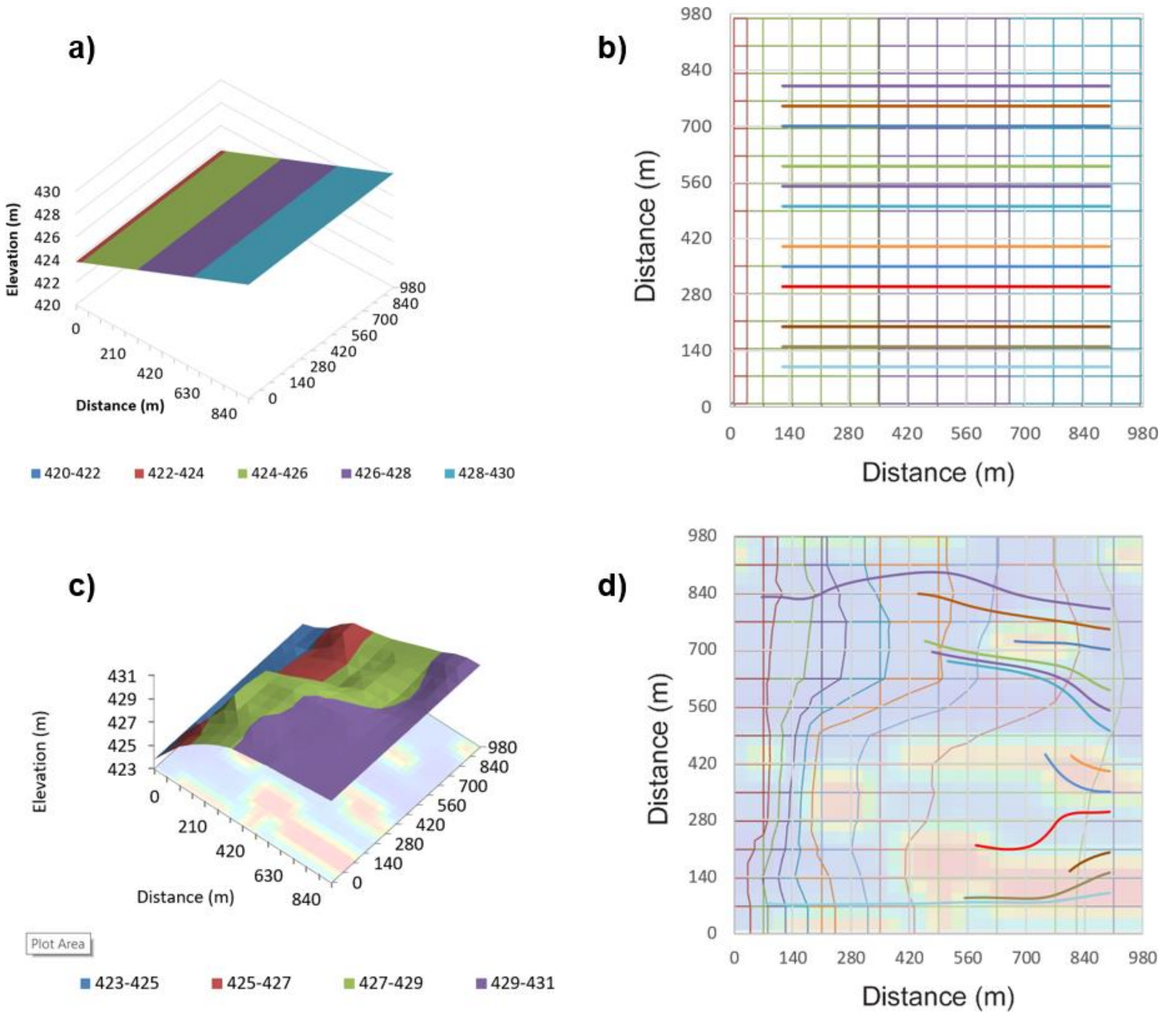

Figure 19 - a) Equipotential surface (with water level contours) for a hypothetical homogeneous flow system with hydraulic conductivity of 2.5 m/d and an overall gradient across the domain of 0.001 causing flow from right to left. b) Traces of 12 particles transported for 40 years (porosity assumed to be 0.3). Note all particles travel the same distance in the same direction, indicating a plume in this setting would remain intact and undergo minimal mixing from causes related to groundwater velocity. c) Same flow system as (a) showing the water level surface in three dimensions for the case where the aquifer is heterogeneous with lenses of *K* ranging from 0.25 (blue) to 25 m/d (red) (shown on the x-y plane). d) The traces of the same 12 particles from (b) released into the heterogeneous flow system shown in (c) for 40 years. Note the variation in particle pathways suggesting considerable plume distortion and splitting, enhancing the conditions that promote mixing at the molecular scale. This effect is solely due to variations in groundwater velocity.

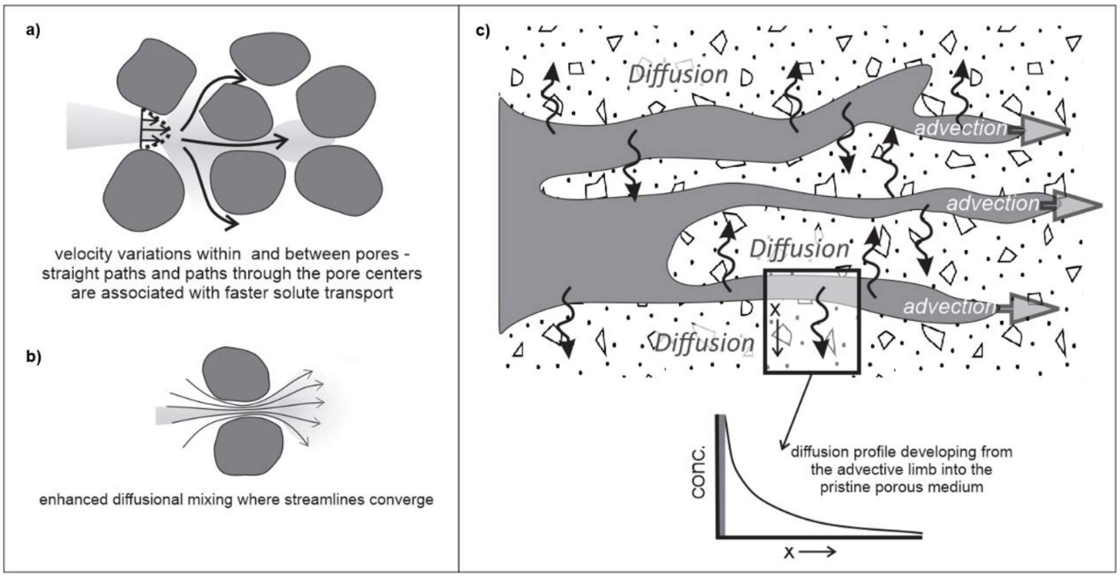

Figure 20 - Historically, dispersion has been visualized as the result of the processes illustrated above. These processes do not directly cause molecular scale mixing, but they can promote it by creating conditions favorable for diffusion. a) Velocity variations may occur within pores, or between pores resulting in enhanced pollutant concentration gradients (i.e., the difference of concentrations at two points divided by the distance between the points, $\Delta C/\Delta x$) in directions transverse to flow. These gradients drive mixing by diffusion, which can occur over short time scales at the pore scale. b) In addition, the compression of streamlines within some pores increase the transverse concentration gradients by decreasing the magnitude of the Δx in the $\Delta C/\Delta x$ term. c) Variations in velocity at larger scales can also create zones with high concentration gradients. In such zones, diffusion occurs at the maximum rates for those scales, and mixing is promoted. Note: the diffusion profile shown is provided to illustrate the tendency for pollutant mass to mix with surrounding groundwater by diffusion. A fully developed diffusion profile such as the one shown would be repeatedly disrupted in a transient flow system, or as a plume evolved, and never be achieved. Velocity variations at the pore scale are important over centimeter lengths or less. Velocity variations at the centimeter scale or higher may be of practical concern for characterization and remedial design purposes.

The link between these two factors begins when a plume distorts, splits or fragments over time due to variations in velocity (e.g., Figure 19c and d) arising from such causes as aquifer heterogeneity, seepage to the ground surface (e.g., seeps, streams, lakes), or pumping. This phenomenon can occur at any scale where the flow variations occur. Once the plume has been deformed in this way, sharp concentration gradients can develop within and around the plume perimeter, leading to enhanced diffusive mixing between the plume and the ambient groundwater (Figure 20). Since diffusive mixing occurs at the molecular scale, any velocity variations that promote it are also drivers of the micro-scale mixing process. This view of mixing in the subsurface is sometimes referred to as the advection-diffusion mechanism.

In general, the geological variations that lead to flow variability and molecular scale mixing occur at scales smaller than the measurement scales used to characterize flow systems, making predictions of mixing rates a challenge. Recent research is re-examining the way dispersion is handled in the advection-dispersion equation and re-assessing the nature of the link between groundwater velocity and mixing rates. Nevertheless, the link itself is not in question. Therefore, the issues, discussed above, that make subsurface mixing important also make groundwater velocity measurement important, at the appropriate scale.

4.4 Groundwater residence times and travel times

The definitions of travel time, residence time and groundwater age provided by other Groundwater Project books (e.g., "Isotopes and environmental tracers as indicators or water sources and flow rates↗") and are discussed in detail there. Nevertheless, they are worth reintroducing here because the terms are commonly used interchangeably to describe the time a parcel of water spends in the saturated zone, and that time can be estimated as an *advective* travel time from the point of recharge to the sampling point, i.e., a time that depends on groundwater velocity. In the context of contaminant fate, transport and remediation, the term 'residence time' might also be used to refer to the time a parcel of water spends in a treatment zone within some limited volume of an aquifer. Regardless, the time that a parcel of water spends in the ground can be immensely important for the fate of its chemical constituents and is strongly affected by groundwater velocity. In keeping with the example of a pollutant as a groundwater constituent, this is true both from the standpoints of 1) pollutant abatement by biotic or abiotic degradation reactions that require a minimum residence time in the aquifer to progress toward completion, and 2) processes that affect the transport-and-storage of pollutants in variably permeable geologic materials. It is useful to discuss these concepts in the context of flow systems, which are — even in the simplest examples — composed of regions of relatively fast and slow flow rates (Figure 21).

The concept of residence time, as it relates to a flow system, can be further illustrated for an advection dominated flow system by recalculating the particle tracks in Figure 21d for a range of travel times and recording the ages of the particles at each final coordinate location. Contours of these ages are referred to as *isochrons*, and for the simplistic model in Figure 21d the isochrons reveal that the oldest water is deepest, and the youngest water is shallow. Moreover, these ages are layered horizontally (Figure 22).

The connection between residence times and chemical transformations exists for any substance that is chemically active, i.e., out of equilibrium. For example, consider a pollutant that undergoes a transformation with a half-life of 7.5 days and suppose that the path-lines in Figure 21d represent 30-day travel times, i.e. 4 half-lives of the pollutant. This residence time is sufficient to reduce the pollutant concentration to about 1/16th of its original value. For practical purposes, 7 half-lives provide a time period sometimes considered sufficient for 'complete' degradation because it reduces the concentration to less than 1% of the original value. Now imagine that four parcels of water containing the pollutant are released on the surface at various locations along the flow system. The track-lines shown in Figure 21d indicate that parcel 4 will travel more than 16 m horizontally and nearly 15 m vertically, reaching the right boundary before the pollutant is degraded to target levels. On the other hand, parcel 1 with about the same 15 m vertical distance travelled but covering no appreciable horizontal distance over the same time period, will experience full degradation by the time it reaches the boundary, about 135 days (~7 half-lives) after release. In this scenario, it might be concluded that there is greater risk associated with the movement of parcel 4 than parcel 1, largely because of its higher velocity. However, this conclusion may change for cases in which the pollutant has longer reaction times or is non-reactive. In that scenario, dissolved contamination from a short-lived spill (instantaneous source) would be flushed from the system more quickly along track 4 than track 1, attaching the greater risk to parcel 1 because of the persistence of the pollutant. Once again, the importance of a detailed characterization of the flow system, particularly through knowledge of groundwater velocities, is fundamental to assessing the fate, transport and risk associated with chemicals carried by groundwater.

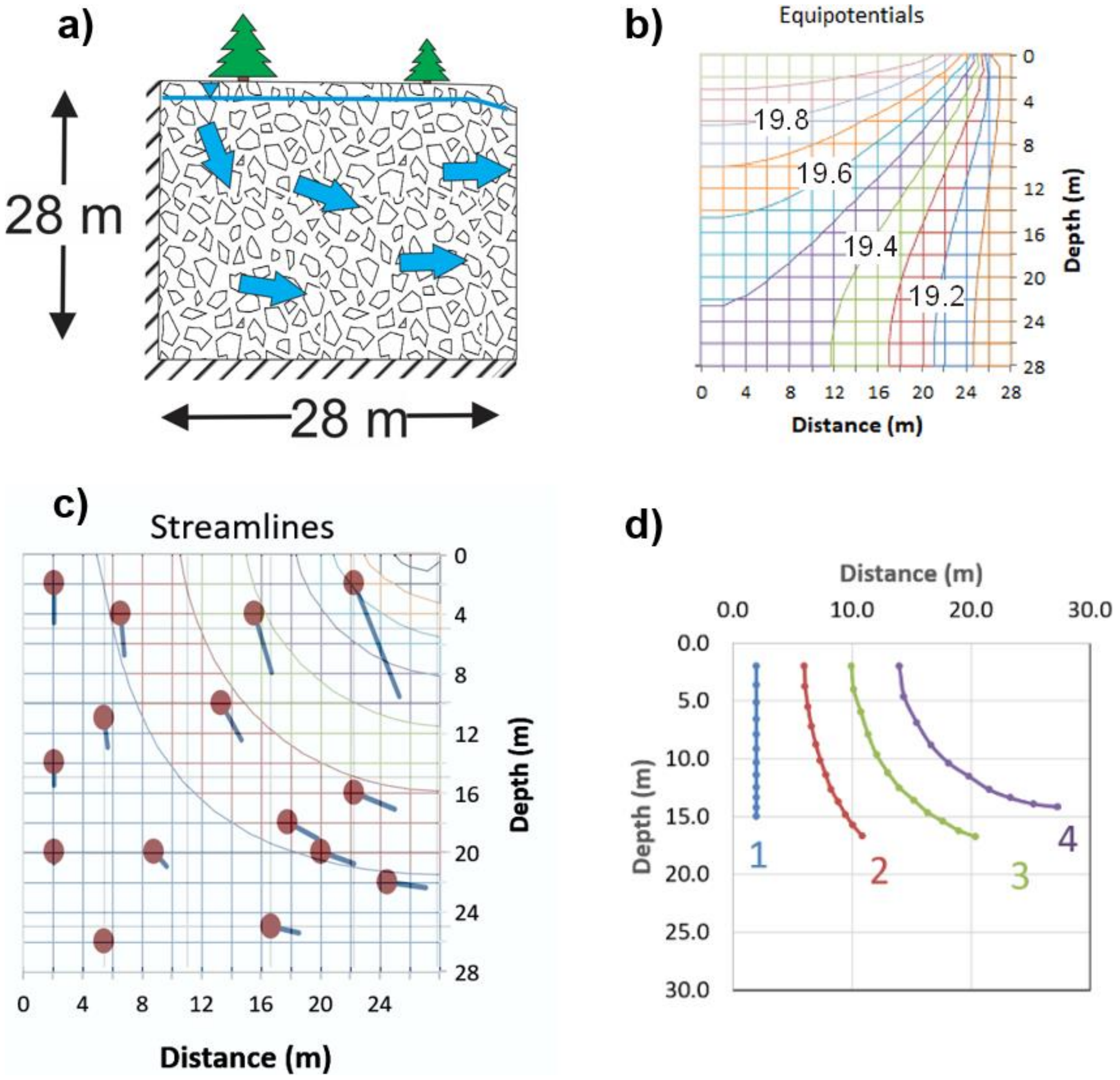

Figure 21 - a) A Cross-section of a simple, homogeneous flow system with a flow divide (no water crosses a divide) on the left and an impermeable base layer. Water recharges from the surface and exits the system at the right boundary. b) Contoured water levels (equipotential lines as elevations in meters) in the aquifer; closer spacing of the lines indicates faster flow. c) Streamlines showing the paths of groundwater flow, and points (red dots) with velocity vectors (blue lines) showing direction of flow and scaled so lines are proportional to the water speed. d) Path lines of four parcels of water originating from different locations in the flow system and traveling for the same period of time. Note that because of its location in the flow system, parcel 4 travels a greater overall distance in the same period of time than parcel 1 — this is particularly evident in terms of the horizontal distances travelled.

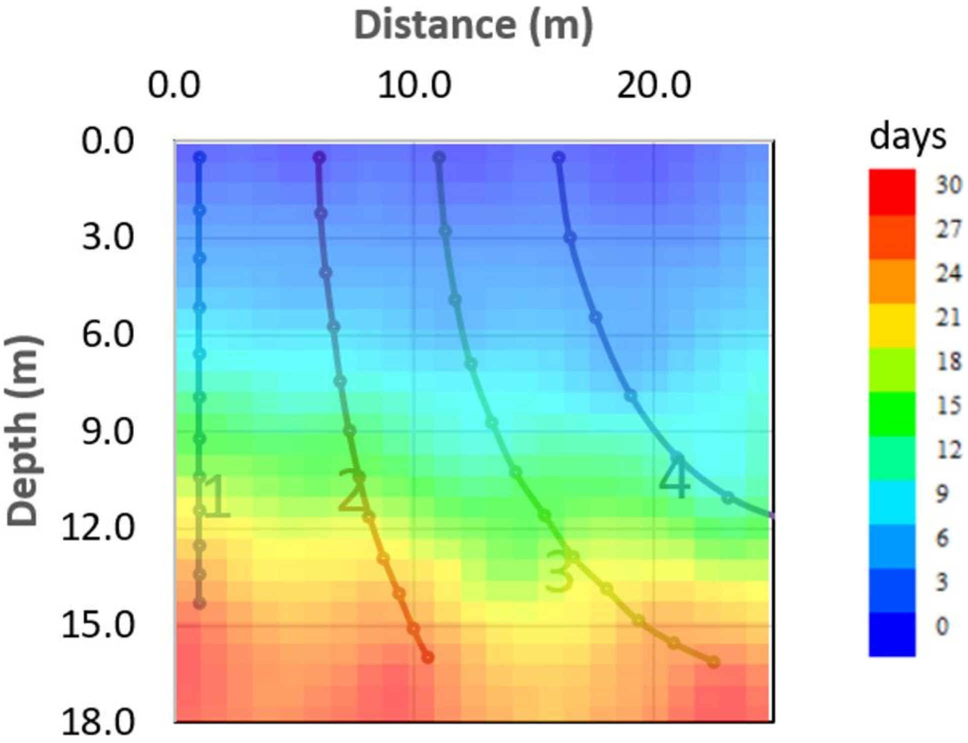

Figure 22 - Cross-sectional view of part of a 30 m by 30 m hypothetical aquifer with 30-day particle tracks and colored isochrons displayed. The calculations performed for this image are approximate, based on the four particles shown and six different times (5, 10, 20, 25, and 30 days), but the near horizontal layering of groundwater ages (or residence times) is also observed in more sophisticated models.

To gain insight into groundwater residence times, hydrogeologists have sometimes relied on the sampling and analysis of tracers. An especially useful family of tracers are the radioactive isotopes. When these are released into the groundwater, either by design or by accident, they serve as tracers with on-board clocks that can be used to estimate water residence times. Isotopes that might be used this way include tritium (^3H, $t½$ = 12.5 years), carbon-14 (^{14}C, $t½$ = 5730 years) or strontium-90 (^{90}Sr, $t½$ = 28.8 years) as discussed by Cook (2020). If there is knowledge of the isotope concentration at the time of its introduction to the ground then, in principle, any subsequent determination of its concentration will be enough to calculate how long it has been there. This assumes ideal conditions, in which other processes that contribute to declines in isotope concentration can be assumed minimal (e.g., dilution or sorption). Knowing the distance between the release location and the sampling location, an average velocity and total residence time (i.e., time between release and sampling) can be estimated. The applicability of this method is strengthened if isotope ratios of parent to daughter compounds are considered. Isotopes have been employed these ways as *in situ* indicators of plume-scale velocities. However, a problem arises when the aquifer being investigated is heterogeneous. Here, the relationship between residence time and transport-and-storage becomes important.

In heterogeneous media — we will consider the case of interbedded sands and clays here, but the following discussion is relevant to other combinations of geologic materials — groundwater will deliver pollutants to the more permeable sand zones first, because the water travels faster there, setting up concentration gradients at the boundaries between the sand and clay (Figure 23). Flow rates in clays are very small and so the transport mechanism that dominates in these materials is diffusion. As a pollutant, or isotope tracer, passes through the sandy material, its plume continuously loses mass to the clays by diffusion, effectively storing mass in the clays until the concentration gradients are reversed. The loss of pollutant mass from the sand-bound plume has the effect of slowing the forward movement of the plume, i.e., contours of a specified concentration advance less rapidly than they would in a homogeneous aquifer. This is important for at least two reasons: first, knowledge of the seepage velocity from Darcy calculations may overestimate the tracer velocities and predict arrival times at receptors that are unrealistically short (note: in cases of severe heterogeneity, the opposite error could occur — strong channelized flow might result in Darcy calculations that underestimate seepage velocities, as illustrated in Figure 23c); second, this mechanism can lead to greater than anticipated residence times for pollutants, potentially fostering greater degrees of degradation if the pollutant is reactive, or simply increasing its time in the ground if the pollutant has low reactivity. Either way, the pollutant mass that would have contributed to a growing plume instead collects in the ground and may be difficult and expensive (with respect time and/or money) to recover in a remediation program.

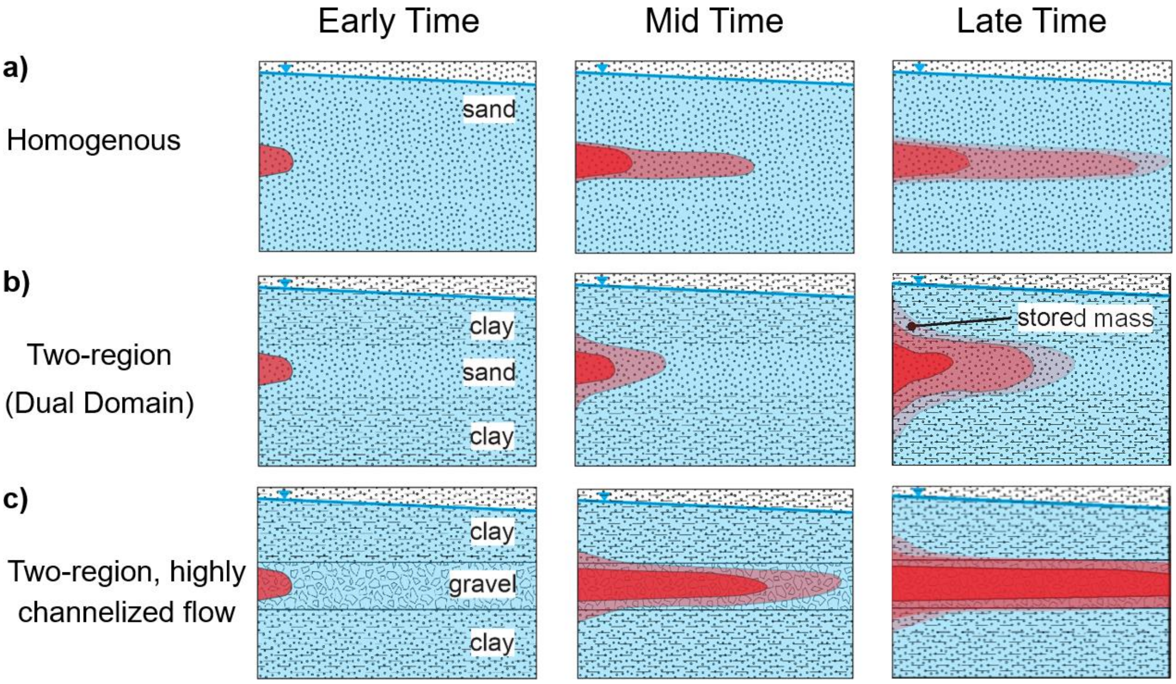

Figure 23 - Conceptualization of plumes being transported in a) a homogeneous sandy medium, b) a heterogeneous medium consisting of sand and clay, and c) a second heterogeneous medium consisting of gravel and clay. Compared to the homogeneous medium, the other two constitute transport in two regions: predominantly advective transport in the sand and gravel layers and mainly diffusive transport in the clay. The effect of the diffusive transport is to store mass and retard the plume compared to the homogenous case. If the clay is coupled with highly permeable sediment (perhaps not known to be present), such as gravel, the advective transport can proceed much faster, overwhelming any retardation that might be expected for the sand-clay coupling

4.5 Contaminant mass discharges

As alluded to in previous sections, real-world aquifers are to some degree heterogeneous. This means that they are composed of geologic materials and structures of different properties that influence flow and chemical constituents. A great concern to hydrogeologists is that the heterogeneity may manifest itself as continuous layers, channels, faults, or other conduits that are highly conductive to flow. When this occurs, flow through these units can be focused and fast enough that mass losses to surrounding less permeable units, via diffusion for example, may be too slow to meaningfully retard a plume front. The delivery of pollutants to down-stream receptors may therefore occur much faster than predicted from conventional Darcy-based characterization methods. Moreover, if the pollutant source is a long-term one, the rate at which mass accumulates at the receptor will also be higher than expected. The combined concerns of time-to-arrival (from knowledge of v and q) and rate of mass delivery are captured in the concept of *mass flux*. Mass flux has dimensions of mass per time per unit cross-sectional area of aquifer (Figure 24).

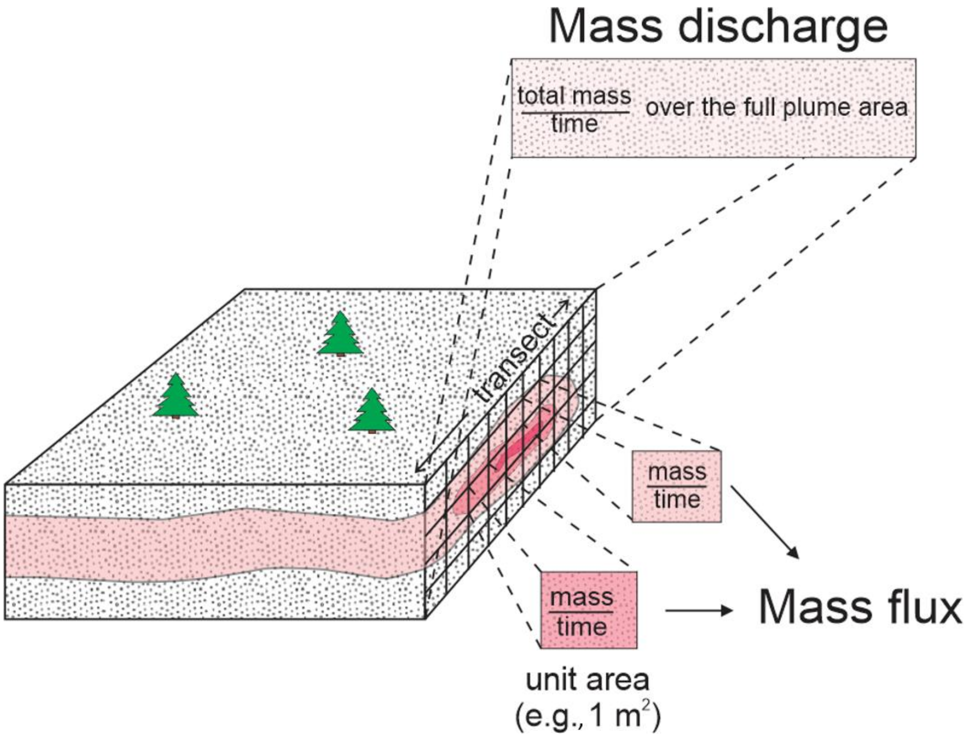

Figure 24 - Relationship between mass flux and mass discharge. Mass flux is the mass of a contaminant that crosses a unit cross-sectional area of an aquifer per unit of time, and it may vary within a plume, as it does between the two example areas shown by the differing colors (dark red and light red). Mass discharge is simply the sum of fluxes over the entire plume

The mass per time portion of a mass flux can be determined by multiplying the observed concentration of contaminant considered representative of a unit area by the Darcy flux (see the introduction of this book). Within a plume, flow rates and concentrations of a pollutant may vary, so the mass flux may also vary from location to location. The total plume mass per time passing through a transect consisting of many unit area sections is calculated simply by adding up the mass fluxes for each unit area in the transect. This value is called the *mass discharge* (dimensions of mass/time).

While mass flux is a number that can be compared across sites, and within sites, because it always references the same amount of area, mass discharge provides a site-specific value that can facilitate risk assessment analysis. A mass flux number can be high but if the total plume area is small, the total mass reaching a boundary or receptor may not pose much risk. On the other hand, large mass discharge is unambiguously problematic in most cases of contaminated sites.

In heterogeneous media, the determination of mass discharge depends on the discovery and characterization of all zones where groundwater velocities are high. A well-instrumented transect, i.e., one with many monitoring points on it, such as the one illustrated in Figure 24, can provide the detail necessary to determine the mass fluxes across the plume — including large fluxes associated with preferential flow pathways — and from them the mass discharge crossing the transect (Einarson and Mackay, 2001).

To illustrate another use of mass discharge for practical purposes, imagine a water supply well that is pumped at a rate *Q* that happens to capture the entire plume of a contaminant known for causing health problems. The people in charge of the water supply might ask if the concentrations that develop in the well will remain dilute enough that the contamination can be ignored, or if there is a possibility that the concentration of pollutant rise to a level that requires action. Prior knowledge of the mass discharge in the plume, together with the pumping rate of the well, permits the needed in-well concentration to be estimated in advance (Figure 25), assuming complete mixing of polluted and unpolluted water in the well.

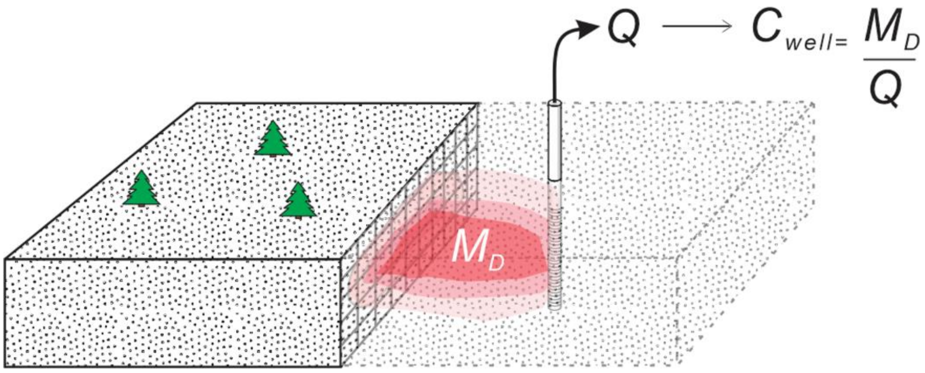

Figure 25 - A plume is captured by a water-supply well. If the mass discharge of a contaminant in the aquifer is known, the concentration that will appear in the well, C_{well}, can be anticipated for any rate of pumping, Q, that captures all of the plume. The simple relationship shows that C_{well} is proportional to M_D, e.g., doubling M_D will double C_{well}.

4.6 Velocity measurements in fractured media

The hydrologic cycle tells us that energy from the sun drives water (primarily) from the oceans into the atmosphere. However, the Earth is not a static planet and eventually conditions prevail that cause the water to rain out of the sky and return to the surface — sometimes the land surface. From there, water seeks the lowest elevation point it can find under the influence of gravity — ultimately returning to the oceans. So relentless is this quest that almost no place that offers space for water molecules is not invaded by them as they make their journey. In the earlier sections of this book, the spaces at issue are those between the grains of sediment or regolith that lie between the sky and the rocky surface of the planet. But the Earth's crust is also a dynamic thing, and the rock that composes it is frequently unable to withstand the tectonic, volcanic, isostatic, or erosional factors that bend, fold, uplift, heat, cool, subside, rotate or weather it. The result is that the shallow rock layers of the planet begin to break up, developing fractures, joints, partings, or solution openings that inevitably fill with water. When the fracturing is sufficiently pronounced, the rock strata can behave as aquifers.

Not surprisingly, the occurrence of fractured rock aquifers is very common. They occur in crystalline, igneous or metamorphic shield rock where the only openings for water are the fractures (Figure 26a), and in sedimentary rocks composed of grains that are consolidated with mineral cements. These rocks exhibit both primary porosity and permeability inherent to the rock matrix, as well as secondary porosity and permeability associated with later fracturing, including partings along contacts between beds (Figure 26b). In cases where sedimentary rock is composed of thick layers of soluble material, such as limestone or dolostone, fractures can become enlarged through dissolution, vastly increasing the capacity to carry water (Figure 26c). This phenomenon underlies the formation of karst topography, a geomorphic descriptor that applies to 25% of the Earth's land surface and which is discussed in greater depth later in this section.

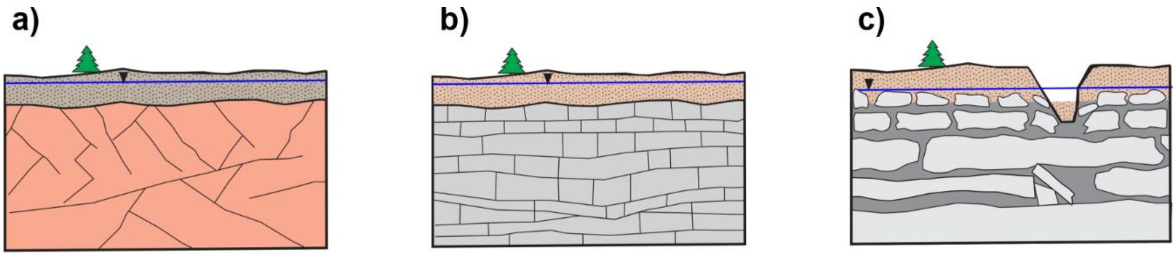

Figure 26 - Conceptual diagrams of three types of fractured rock. a) fractured crystalline rock with relatively low aperture openings associated with faulting, jointing, and fracturing from regional or local tectonic activity, or other geologic processes. b) sedimentary rock with openings associated with bedding planes or fracturing due to local or regional tectonic activity or other geologic processes. c) highly weathered rock such as karst with openings ranging from micron sized apertures to cave conduits, and collapse features like sinkholes that allow surface water to rapidly enter the subsurface.

The application of conventional Darcy's Law approaches to characterize fractured rock aquifers is commonly used but subject to misleading outcomes. In the simplest cases, the density of fractures is very high i.e., fracture spacings are hundreds or thousands of times smaller than the spatial scale of the investigation and the aquifer behaves much like an equivalent porous medium (EPM), so the use of Darcy’s Law is well founded (van der Kamp, 1992). The EPM assumption is also appropriate in cases where the rock matrix has high permeability and does not depend on the fractures to conduct flow. Permeable matrix rock is susceptible to invasion by pollutants due to slow advective flow or diffusion between the fractures and the matrix. This aspect of the fractured media problem is qualitatively similar to Figure 21 and discussed in more detail elsewhere in the Groundwater Project books. Here, the focus is on flow in the fractures.

In many cases involving the investigation of groundwater pollution, the scale of the site is not sufficiently large, compared to the fracture spacing, to support the use of velocity measurement methods that depend on the EPM assumption (Figure 27). In these cases, a form of Darcy’s Law (derived from the ‘Cubic Law’ that relates flow in a fracture to the cube of its aperture) might still be applied for single fractures or fracture sets within a defined section of a borehole. To apply such methods, detailed hydraulic testing of the fracture interval is required, in part to estimate the fracture hydraulic conductivity, K_f, hydraulic aperture, $2b$, and fracture porosity, n_f. It is worth noting that the application of Darcy’s Law in granular media, porosity is in the range of 0.2 to 0.5 while in fractured rock the range extends to much lower values, typically 10^{-5} to 10^{-3} (Morris and Johnson, 1967). Using Equation 3 of Figure 27 leads to an estimated seepage velocity orders of magnitude higher in fractured media than granular media, with important implications for the assessment of risk. This responsibility should not rest entirely on the shoulders of Darcy’s Law since the parameters used in the calculation come with substantial uncertainties. Independent measurements of velocity are highly desirable to validate the Darcy predictions.

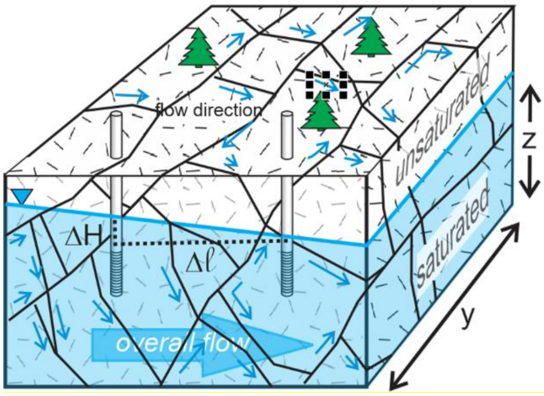

Bulk flow, flux and velocity

$$Q = -KA\frac{\Delta H}{\Delta \ell} \qquad (1)$$

$$q = -K\frac{\Delta H}{\Delta \ell} \qquad (2)$$

$$v = -\frac{K}{n_e}\frac{\Delta H}{\Delta \ell} \qquad (3)$$

Figure 27 - Conceptual diagram of a fractured rock aquifer showing the difference between flow constrained by the fractures (small blue arrows) and the estimated bulk flow from conventional Darcy’s Law calculations (large blue arrow). On a sufficiently large scale, the Darcy calculations will match the average overall flow in the aquifer, including flow direction. On the scale of this diagram severe deviations from the Darcy predictions are evident (small blue arrows) due to locally variable fracture porosity, hydraulic conductivity, and available pathways for flow (also illustrated in Figure 28).

Building on the issues raised above, fractured aquifers pose special challenges for hydrogeologists because unlike granular aquifers, the openings that conduct water behave as discrete pathways rather than a continuous medium. A given borehole — which can be very expensive to drill — may or may not intersect a productive fracture or fracture set, while a second borehole a meter away yields abundant water. Furthermore, not all fractures are created equal; some may have apertures smaller than the width of a human hair while others may be hundreds of microns wide, leading to vast differences in water productivity. In the case of karst aquifers, open channels large enough for a person to enter (i.e., caves) may be present and control the speed and direction of water flow. All of this can add up to counterintuitive water level data when Darcy's Law-based surveys are undertaken with a conventional porous medium mindset. For example, the discrete distribution of fractures can cause the local flow directions to vary widely from regional trends (Figure 27). Water is restricted to flow through the available openings whether or not they align with predictions based on Darcy's Law (Figure 28a).

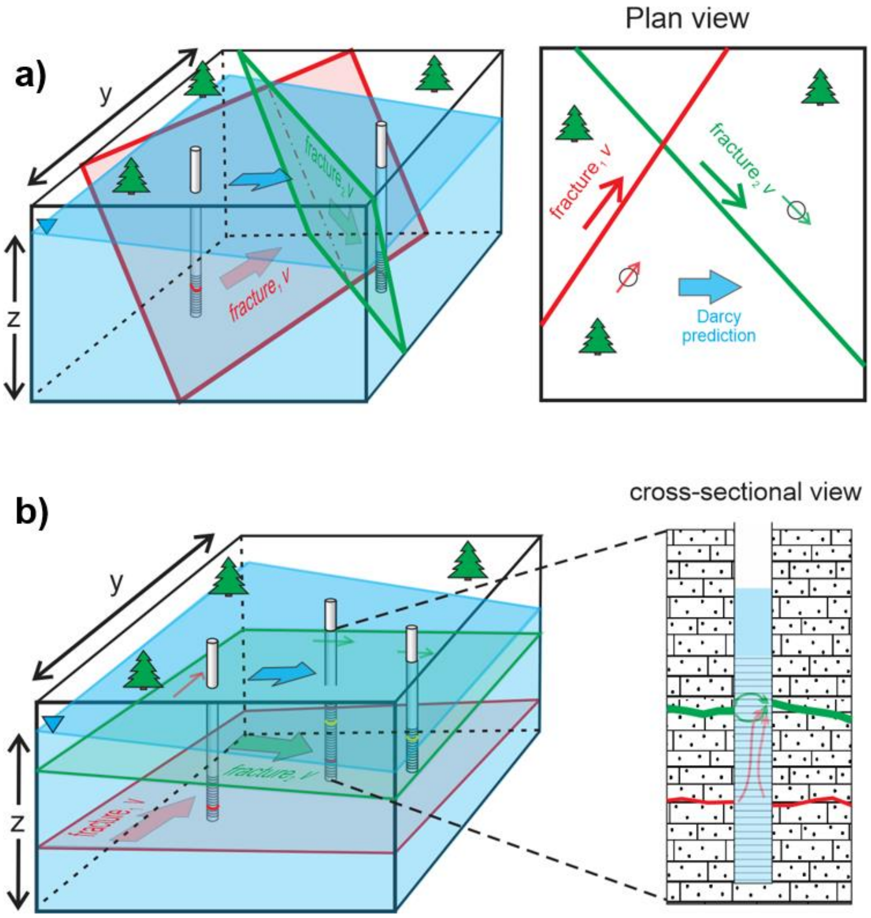

Figure 28 - Simplified schematics of two fracture systems in which the matrix rock is practically impermeable. a) intersecting fractures each with its own flow magnitude and direction, determined by the respective orientations of the fractures, neither of which corresponds to the regional flow determined from Darcy's Law. b) Non-intersecting fractures in hydraulic isolation except for a cross-cutting borehole. The two fractures have different flow directions and magnitudes, with the upper fracture dominant. Flow enters the borehole from the lower fracture and leaves the borehole through the upper fracture making the measurement of horizontal velocity in the open well problematic.

The importance of this insight is illustrated with the following hypothetical scenario: a receptor (e.g., a water supply well) is apparently off the path of contaminant transport according to conventional determinations of hydraulic gradient and appears safe from pollution emanating from a buried tank. However, the receptor draws its water from the same fracture carrying polluted groundwater from the leaking tank. Without knowledge of the flow direction in the fracture, it is difficult to assess the risk to the receptor.

A special case that falls into the category of rock-aquifers is karst, as mentioned earlier in this section. In addition to the issues raised above, karst landscapes are characterized by large solution voids in the underlying rock that can conduct subsurface water in what are essentially channels. This can lead to uncharacteristically high (for groundwater) linear velocities that reach magnitudes approaching kilometers per day (Figure 29). Therefore, tools used for porous media or fractured rock, which typically conduct water at lower velocities, may not be suitable for measuring the high flow rates in some karst settings. A favored method for determining groundwater velocity in karst settings is dye tracing (Aley, 2002). These tests are conducted by introducing fluorescent dyes (most commonly) into sinkholes or other recharge locations and monitoring downstream springs for the appearance of the dyes. The success of the method depends in large part on the low detection limits (parts per trillion range) possible with the fluorescent dyes. The method is most commonly used to identify overall directions of flow and *times of first arrival* of the dyes at the springs. Details of the pathways taken between the sources and springs are not generally discoverable by this method. Also, average linear velocities, based on the travel time of the tracer center of mass, are not be possible to determine in many cases; the range of tracer mass balances (mass detected at springs/mass released) is <1% to nearly 100%, with a median value of about 5% (Tom Aley, personal communication). The most successful tests for achieving tracer mass balances are those involving flow through a single ‘pipe’, or similarly simple pathway. The poorer mass recoveries are thought to result from a combination of dilution in the subsurface channels, where turbulent mixing is possible, and distributary drainage that occurs in many karst systems. Loss of tracer mass to the rock matrix is also possible where the primary porosity of the matrix is notable, as in many clastic sedimentary rocks. Also, in some cases, tracer loss to biotic or abiotic transformations can occur, though the dyes are usually selected to minimize this possibility over the time period of a test (hours to weeks).

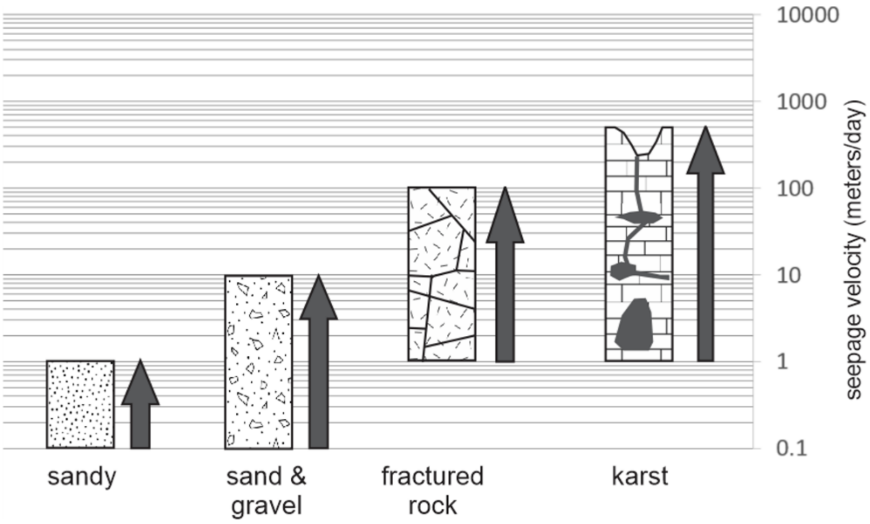

Figure 29 - Approximate, typical seepage velocity ranges for various aquifer settings (John Cherry, Tom Aley, personal communication, 2020). Site specific conditions can extend these ranges for individual cases.

Neglecting karst settings for a moment, fractures in rock tend to be micron-scale openings and are therefore incapable of conducting large water flow on an individual basis (note that fracture sets may cumulatively conduct volumes of groundwater that rival porous media aquifers). However, what they lack in volume they can make up for in speed. The small aperture of a fracture behaves like the small space between the thumb and the hose in Figure 4, so transport rates in fractures can be surprisingly high — many meters per day. As a result, the time between a pollutant release and a detection at a receptor can be grievously small, leaving relatively little time to take preventative or reactive measures.

Another challenge encountered in fractured media is the inadvertent creation of new flow paths by boreholes that intersect hitherto isolated fractures (Figure 28b). These kinds of unintended connections can spread pollutants from contaminated zones to clean zones, as well as obscure the ambient flow directions and magnitudes in the aquifer(s) (Sterling et al., 2005). Moreover, even without interconnecting boreholes, fractures that are hydraulically inactive or dry under normal (average) conditions can become hydraulically active at times when recharge rates are high and water levels in the ground rise — for example, after rainstorms. This can result is unexpected changes in directions and rates of pollutant migration compared to those observed under 'normal' conditions.

The challenges are formidable, but methods are available — and new methods are being developed or adapted — to take on those challenges. As mentioned above, a favored and well-established method to investigate transport in fractured systems or karst is the introduction of tracer dyes near suspected source areas and the monitoring of their breakthroughs at selected points downstream, commonly at natural springs, but also in wells, and discharge zones in streambeds or lakes. Dye tracing is most effectively used to identify preferred flow paths, which is ideally suited for assessing pathways in fractured rock aquifers. The method circumvents the assumptions implicit in Darcy's Law calculations and addresses three primary questions (Aley, 2002): 1) where is the groundwater going? 2) how long does it take to get there? 3) what happens to solutes (substances dissolved in groundwater) along the way? Unfortunately, as mentioned previously, the known mass of tracer released to the subsurface is rarely recovered at the discharge locations, so large fractions of the tracer have unknown fates. In general, the larger the scale of the tracer test, the lower the fraction of tracer mass recovered. Nevertheless, much information can be gleaned from these tests. Question 1 is answered on the basis of which monitored points detect tracer, and question 2 is addressed on the basis of the time of first detection at each of these points. The answers to these questions will tend to be most influenced by the highly conductive pathways in the aquifer, which may be advantageous in many circumstances but will not identify mechanisms by which, or locations where, the tracer (and thus the pollutant) mass collects. Answering the third question can help in this respect. One strategy for addressing question 3 is the inclusion of multiple tracers in a test, each with unique transport characteristics, including partitioning into organic liquids such as petroleum products, solvents (collectively known as non-aqueous phase liquids, or NAPL), and comparing the timing and mass recoveries of the various tracers at the sampling points (Geyer et al., 2007).

The most recent developments for direct measurement of groundwater flux or velocity in fractured media tend to be borehole methods. Advances in borehole geophysical methods are relevant to measuring groundwater velocity in fractured rocks advances but are outside the scope of this discussion. These borehole tools, many of which have been introduced in the earlier sections of this book, are particularly well suited for fractured rock characterization when they can isolate individual fractures, or closely spaced fracture sets, for testing. The IWPVP is an example of a tool that can be deployed to focus on specific, small scale features like these. Also, borehole dilution methods can focus on individual fractures, if used in conjunction with packers. The PFM was redesigned to become the FRPFM by infusing fluorescent tracers into an elastic, inflatable fabric that is held in place in a borehole between packers. The device is emplaced at depths corresponding to fracture locations and the flow from the fractures leaves a visible record, under ultra-violet light, where the tracers are leached from the fabric.

FLUTe™ liners offer some interesting opportunities for fractured rock aquifer characterization (Figure 30). The FLUTe liner is a sleeve that is installed in a well effectively sealing the borehole and preventing cross-depth flow (Keller et al., 2013). Pressure profiles gathered as the sleeve is installed can provide insight into the depths and transmissivities of fractures. If temperature sensing equipment is emplaced outside the liner prior to installation, depths where temperature variations occur indicate water flow and fracture locations. Either thermistors or optical cable (distributed temperature sensing, DTS) can, in principle, be used to gather such temperature profiles.

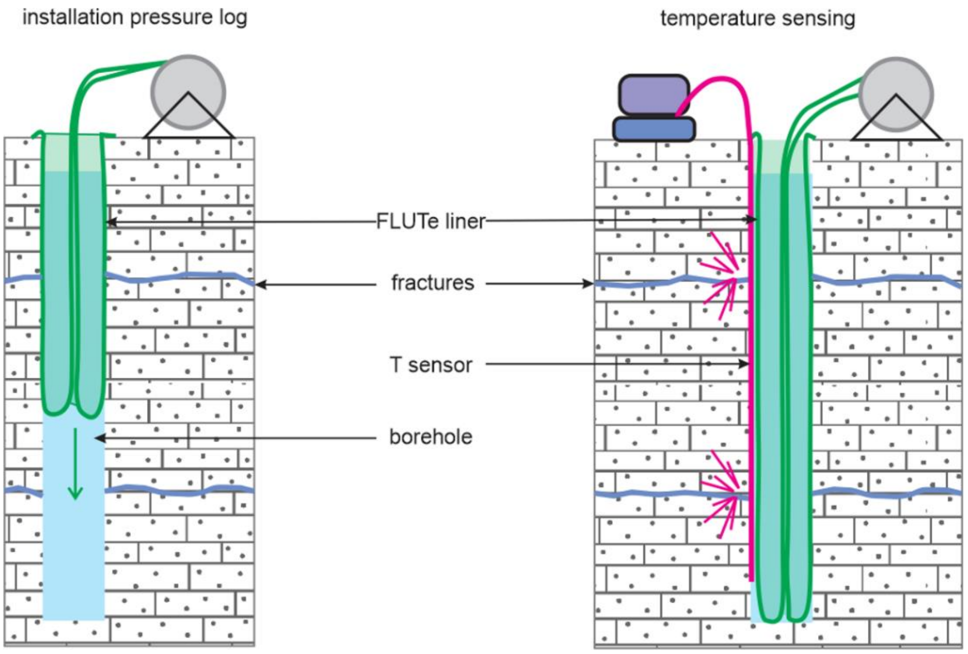

Figure 30 - Schematic of the FLUTe liner as the basis for characterizing fractured media. Both pressure profiles and temperature profiles (using T-sensors) can be used to identify the locations of fractures. The determination of flow rates in the fractures is a further goal for the technology.

A summary of selected technologies used to characterize groundwater flux and velocity in fractured rock direct is provided by Table 2.

Table 2 - Summary of selected technologies used to characterize groundwater flux and velocity in fractured rock.

Method	Scale	Examples	Instrumentation/Description
Darcy-based methods	• generally, ~10 m to ~100m separation between wells • local to regional investigations common • risk of misleading interpretation unless the equivalent porous medium (EPM) assumption is validated	• conventional site investigation based on water level survey and estimation of hydraulic conductivity (*K*)	• wells and water level tapes or sondes • measure head in wells for gradient across domain and obtain domain K value - data collection requires minutes per well • packer testing may be performed to characterize hydraulic properties of fractures to support Darcy calculations
Tracer tests	• meters to kilometers	• dye tracers (Aley, 2002)	• tracer poured into well or recharge site • tracer detected by water sampling or with passive solid sorbent samplers
		• isotopes (Cook, 2020)	• active injection followed by water sampling • sampling only following tracer introduction by spill or natural source
		• salts (Luhmann et al., 2012)	• active injection followed by water sampling
		• colloids (McKay et al., 2000)	• active injection with a two-well injection-withdrawal system
		• dissolved gases (e.g., He, SF_6) (Gupta et al., 1994; Vulava et al., 2002)	• active injection followed by water sampling
Single borehole techniques	• centimeter-scale measurements geared to locations where fractures cross the borehole • larger scale flow patterns possible with multiple wells and complimentary information from other methods	• borehole dilution and FVPD (Brouyere et al., 2008)	• packers to isolate the borehole section of interest, tracer injection system, sampling/datalogging
		• Flute liner • pressure log • temperature profile (Peheme et al., 2010)	• pressure profiling during installation can identify depths of major fractures • temperature profiling next to liner to identify zones of high water-flux - with heating and subsequent return to background temperatures, flow rates may be inferred
		• FRPFM (fractured rock PFM) (Levison and MacDonald, 2014)	• instrument supplied by vendor, suspended in well for days to weeks, packer system required • return to vendor for analysis
		• ORP (oxidation-reduction profiling) • (Sale *et al., 2020)*	• sensors suspended in borehole and passively sense variations in water redox chemistry with depth - depths of greatest variations suggest depths of water flux from fractures • requires datalogger for longer-term data collection
		• IWPVP • (Osorno et al., 2018)	• instrument positioned across fracture for testing • requires injection system and datalogger

5 Summary

The study and characterization of contaminated sites, usually with the aim of deciding upon, designing, and later implementing remedial actions — or settling on the natural attenuation mechanisms to achieve cleanup — depends on a good understanding of the mechanisms that cause pollutant transport and attenuation. This has led to much emphasis being placed on processes involving microbiological activity and abiotic chemical reactions in the subsurface, including those that merely retard contaminant movement without transforming the chemicals. However, none of these factors is sufficient to predict contaminant spreading in the ground unless they are combined with a realistic understanding of the site-specific flow system. Typically, Darcy's Law has been the basis for describing flow systems. The approach is to measure water levels in at least three wells, and from this determine a hydraulic gradient and flow direction. Hydraulic conductivity is then estimated either by laboratory or field techniques — and usually with a notable uncertainty attached to it — and a Darcy flux is calculated. Seepage velocities are subsequently estimated with the additional consideration of the effective porosity. Furthermore, the spacing between wells in these types of investigations often leads to spatial averaging of the flow variations in the subsurface. This methodology has proven effective enough over several decades that alternative methodologies have been used only sparingly. Our modern understanding of contaminant hydrogeology has revealed the ubiquity and importance of subsurface heterogeneity. There is gaining appreciation that aquifers are challenging to characterize with conventional methods that are usually applied at scales of tens of meters or greater. In a field that depends on the identification and treatment of pollutants in concentrations as low as parts per trillion, a very detailed knowledge of the prevailing flow system is highly advantageous if cleanup efforts are to have a chance of succeeding. Perfect knowledge of biodegradation rates, mineral reactions, and sorption are all insufficient to predict contaminant fate and transport, mixing rates, mass discharges, or consumption of aquifer buffering capacities unless groundwater flow velocities are also well known.

The technologies developed to compliment conventional Darcy-based studies tend to rely on tracers to infer the nature of flow. These may be implemented using multiple wells, as in inter-well tracer tests, or single wells, such as is the case with point dilution methods, passive flux meters, heat pulse flowmeters, passive flux meters, colloidal borescopes, or in-well point velocity probes. A subset of technologies advocate deployment of instruments in direct contact with the aquifer material, within dedicated boreholes, to avoid complications and flow distortions associated with filter packs and well screens. The 'direct contact' requirement of these instruments currently limits their use to aquifers that will collapse against them, i.e., those comprising unconsolidated, non-cohesive porous media. Two examples of such technologies are the In Situ Permeable Flow Sensor (ISPFS) and the Point Velocity Probe (PVP).

Many of the tools under development for small scale velocity measurements in porous media may be adaptable for use in fractured media as well. Fractured media pose a variety of special challenges for aquifer characterization studies. These include the identification and characterization of important conduits for flow, and the determination of flow directions that can deviate substantially from those predicted by water level maps. Traditionally, the Darcy approach is reliable if an EPM assumption is justified. Otherwise, tracers are effective to gain large scale pictures of where water flows and the lengths of transit times. Tracers can also be effective in smaller scale studies, but here they compete with single borehole tests that may be less expensive and arguably more controlled. The single borehole techniques that can be adapted to measure small intervals in a borehole are the ones best positioned to shed light on transport in fractured media. These technologies range from instruments that measure flow in single fractures to those that can characterize an entire borehole in a single operation.

Contaminant hydrogeology is an applied field that depends on many sciences and coaxes them to “play together” nicely. The overarching rules that ensure these playmates are harmonious are those that govern where, and how fast, the groundwater moves. The future promises to provide us with tools that will make observations of flow systems in time and space more detailed and affordable than ever before. This prognosis bodes well for the future of hydrogeology and our ongoing endeavors to reclaim contaminated aquifers.

Exercises

To work these exercises, download the interactive Microsoft-Excel spreadsheet titled "**GWP_Velocity_Exercises.xlsm**" as well as the exercise solutions in the spreadsheet titled "**KeyFile_GWP_Velocity_Exercises.xlsm**" from the gw-project.org website on the Groundwater Velocity book page↗. When opening the spreadsheet, you may receive a message about enabling content, updating content, or circular references. Proceed by clicking enable content, not updating content, and clicking OK for circular references. You may wish to save the sheets under another name to preserve a copy in its original condition while working in a revised copy. The KeyFile_GWP_Velocity_Exercises spreadsheet includes the questions and exercises of the GWP_Velocity_Exercises spreadsheet as well as the solutions.

Exercise Set 1

If you have not already downloaded the spreadsheets for the exercises and their solutions that are presented in this book, you can do so at the gw-project.org website on the Groundwater Velocity book page↗ by downloading the interactive Microsoft-Excel spreadsheets titled "**GWP_Velocity_Exercises.xlsm**" and "**KeyFile_GWP_Velocity_Exercises.xlsm**".

1. Open the spreadsheet "GWP_Velocity_Exercises.xlsm". You may receive a message about enabling content, updating content, or circular references. Proceed by clicking enable content, not updating content, and clicking OK for circular references. Then click on the tab for 'Exercise 1'. Consider the simplified porous medium shown. Just as aquifers composed of sediment grains are imperfectly packed, this cartoon displays empty spaces between the grains (blue in Figure Exercise 1-1a). In the spreadsheet, drag the individual grains from the 'real' porous medium to the empty vessel illustrated in Figure Exercise 1-1. Stack the grains with no space between them (*that is,* finish the process started in Figure Exercise 1-1c). Assume that the area of each grain is 4 square units.

   What is the fraction of open space to total space, i.e., the total porosity, in the porous medium?

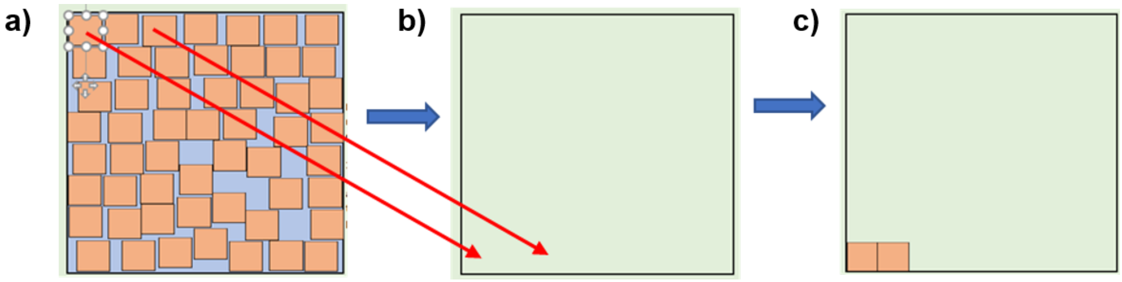

Figure Exercise 1-1 - a) Imperfectly packed grains of an aquifer sample are to be moved into panel b) the total space of the sample so that in c) they are stacked in a closely packed arrangement.

***The solution for Exercise 1-1** begins on row 6 of the Solutions Tab of KeyFile_GWP_Velocity_Exercises.xlsm*

2. Now, scroll down in the spreadsheet to look at the porous medium with ovate grains on row 24. Each of these grains has the same area as the square grains in question 1 of Exercise Set 1.

   What is the total porosity for this medium? Justify your answer on a purely qualitative argument (no calculations).

   Ovate grains can isolate pockets of the 'aquifer' space - *i.e.*, pores. Count the number of isolated pores. For the purposes of this exercise, allow single isolated pores or pairs of pores in isolation to constitute 'dead end' pores. Three or more connected pores do not represent dead ends. It might help the process to color the dead-end pores as shown in Figure Exercise 1-2).

Assuming each pore has an area of 1 square unit, subtract the area of dead-end pores from the total open space area and recalculate the porosity.

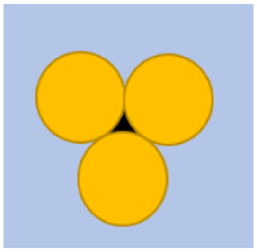

Figure Exercise 1-2 - Example of coloring in a closed pore.

This recalculated porosity is called the *effective porosity* since it represents the porosity capable to transmitting water.

***The solution for Exercise 1-2** begins on row 27 of the Solutions Tab of KeyFile_GWP_Velocity_Exercises.xlsm*

3. Scroll further down the spreadsheet and consider the porous medium with two sizes of ovate grains. Drag all of the small grains (1 square unit each) and place them in the spaces between the large grains (4 square units each) in the neighboring 'aquifer'. This is analogous to making the medium less well sorted.

   Recalculate the total and effective porosities with the small grains added to the porous medium. Compare both with the answers obtained in (1) and (2) and explain the reasons for any differences.

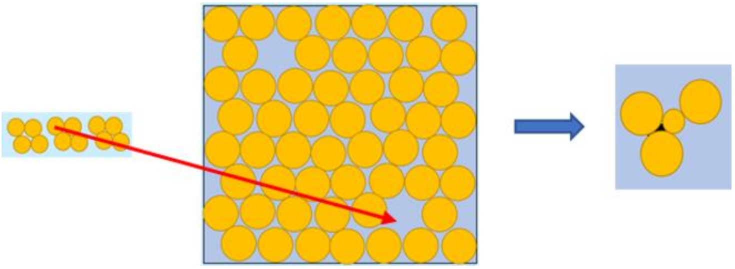

Figure Exercise 1-3 – Drag the small grains into the sample to fill in pores between the larger grains and color in pores that are disconnected from the other pores.

***The solution for Exercise 1-3** begins on row 48 of the Solutions Tab of KeyFile_GWP_Velocity_Exercises.xlsm*

Exercise Set 2

If you have not already downloaded the spreadsheets for the exercises and their solutions that are presented in this book, you can do so at the gw-project.org website on the Groundwater Velocity book page↗ by downloading the interactive Microsoft-Excel spreadsheets titled "**GWP_Velocity_Exercises.xlsm**" and "**KeyFile_GWP_Velocity_Exercises.xlsm**".

1. Consider the conceptualized diagram of an aquifer shown in Figure Exercise 2-1. A lucky hydrogeologist placed two wells in the ground at this site and somehow aligned them perfectly with the flow direction. As a result, these two wells are all that are needed to estimate the Darcy flux and seepage velocity in the aquifer.

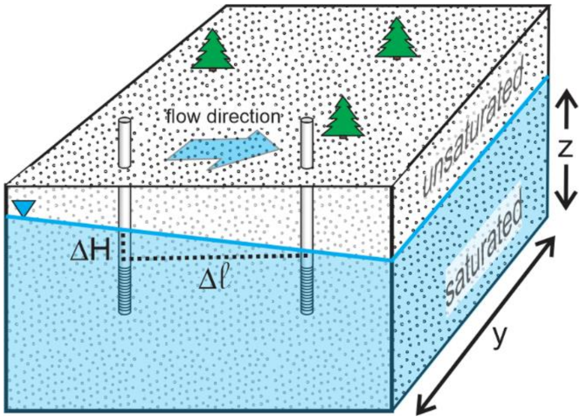

Figure Exercise 2-1 - A lucky hydrogeologist placed two wells in the ground at this site that are aligned perfectly with the flow direction.

Open the spreadsheet "GWP_Velocity_Exercises.xlsm". You may receive a message about enabling content, updating content, or circular references. Proceed by clicking enable content, not updating content, and clicking OK for circular references. Then click on the tab for 'Exercise 2'. Note that the wells are 20 m apart (Δℓ) with a difference in water levels between them of 0.02 m (ΔH). Prior work in the wells led to an estimate of $K = 20$ m/d for the aquifer. The sediments are dominantly sand, and the effective porosity (n_e) is estimated to be 0.28.

Given the equations for Darcy flux and seepage velocity given on the Exercise 2 sheet, calculate these quantities in the space provided on the sheet.

***The solution for Exercise 2-1** begins on row 71 of the Solutions Tab of KeyFile_GWP_Velocity_Exercises.xlsm*

2. Scroll down to row 31 and consider the conceptualized diagram of an aquifer as shown in Figure Exercise 2-2. In this case a more experienced hydrogeologist placed three wells in the

ground, confident that no matter what the flow direction, it could be determined, so no luck would be required.

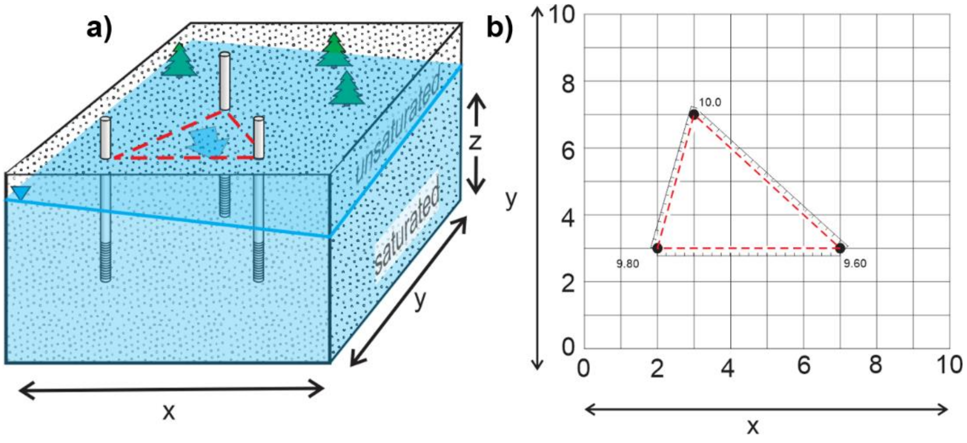

Figure Exercise 2-2 – A conceptualized diagram of an aquifer with a) three wells used to investigate the site in order to estimate both the direction of flow and the velocity; and, b) a map showing the relative positions of the wells and the water level elevation in each well.

The scales (arbitrary units) provided on the map of Figure Exercise 2-2b and in the Exercise 2 tab of the "GWP_Velocity_Exercises.xlsm" spreadsheet can be used to determine the distance between the wells.

Prior work in the wells led to an estimate of K of 20 m/d for the aquifer. The sediments are dominantly sand, and the effective porosity (n_e) is estimated to be 0.28.

Use graphical construction to determine the flow direction, relative to North (north is aligned with the positive direction of the y-axis), and the hydraulic gradient by interpolating to find the location of 9.8 between the north and east well, drawing a line from that point to the west well and constructing a perpendicular to that line from the north well.

Given the equations for Darcy flux and seepage velocity provided on the Exercise 2 sheet, calculate these quantities for the system of Figure Exercise 2-2 in the space provided on the sheet.

***The graphical solution for Exercise 2-2** extends from row 97 to row 114 of the Solutions Tab of KeyFile_GWP_Velocity_Exercises.xlsm*

Item 3 below describes a mathematical versus graphical approach to solving a three-point problem.

3. There are several ways to solve the three-point problem, but one way that lends itself to finding the gradient (and its direction) of a water table with three wells, or more, involves matrix algebra as shown in Figure Exercise 2-3.

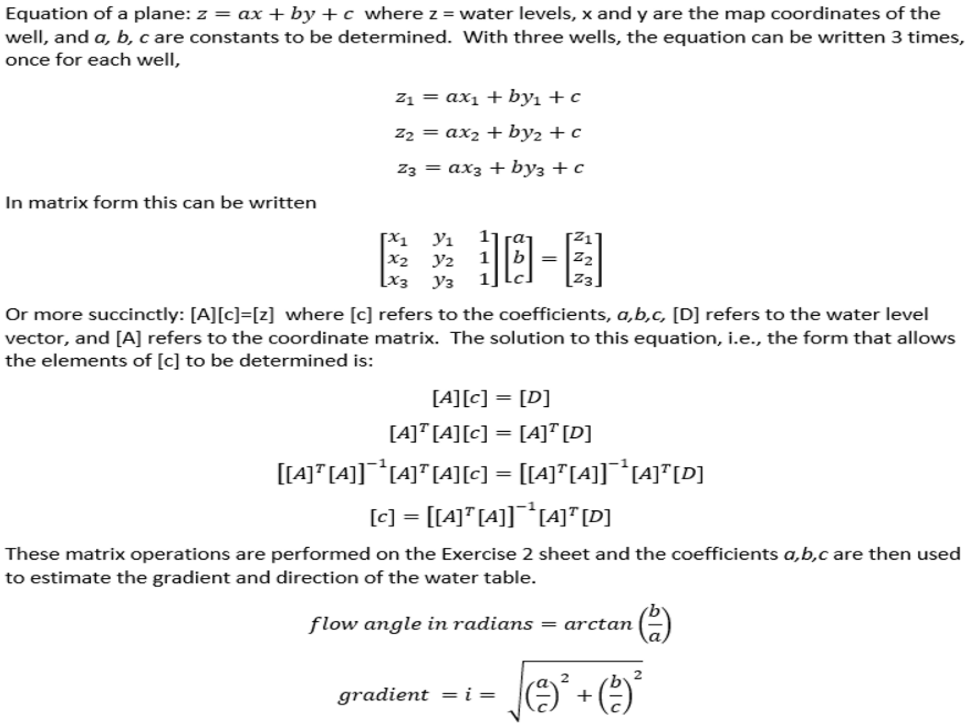

Equation of a plane: $z = ax + by + c$ where z = water levels, x and y are the map coordinates of the well, and *a, b, c* are constants to be determined. With three wells, the equation can be written 3 times, once for each well,

$$z_1 = ax_1 + by_1 + c$$
$$z_2 = ax_2 + by_2 + c$$
$$z_3 = ax_3 + by_3 + c$$

In matrix form this can be written

$$\begin{bmatrix} x_1 & y_1 & 1 \\ x_2 & y_2 & 1 \\ x_3 & y_3 & 1 \end{bmatrix} \begin{bmatrix} a \\ b \\ c \end{bmatrix} = \begin{bmatrix} z_1 \\ z_2 \\ z_3 \end{bmatrix}$$

Or more succinctly: [A][c]=[z] where [c] refers to the coefficients, *a,b,c,* [D] refers to the water level vector, and [A] refers to the coordinate matrix. The solution to this equation, i.e., the form that allows the elements of [c] to be determined is:

$$[A][c] = [D]$$
$$[A]^T[A][c] = [A]^T[D]$$
$$\left[[A]^T[A]\right]^{-1}[A]^T[A][c] = \left[[A]^T[A]\right]^{-1}[A]^T[D]$$
$$[c] = \left[[A]^T[A]\right]^{-1}[A]^T[D]$$

These matrix operations are performed on the Exercise 2 sheet and the coefficients *a,b,c* are then used to estimate the gradient and direction of the water table.

$$flow\ angle\ in\ radians = arctan\left(\frac{b}{a}\right)$$

$$gradient\ = i = \sqrt{\left(\frac{a}{c}\right)^2 + \left(\frac{b}{c}\right)^2}$$

Figure Exercise 2-3 Use of matrix algebra for solving a three-point problem to find the magnitude and direction of the hydraulic gradient of a water table with three, or more, wells.

Open the spreadsheet "GWP_Velocity_Exercises.xlsm". You may receive a message about enabling content, updating content, or circular references. Proceed by clicking enable content, not updating content, and clicking OK for circular references. Then click on the tab for 'Exercise 2' and fill in the table starting near row 69 to verify the graphical solution you obtained for Exercise Set 2, #2.

Given the equations for Darcy flux and seepage velocity given on the Exercise 2 sheet, calculate these quantities in the space provided on the sheet.

***The solution for Exercise 2-3** extends from row 116 to row 164 of the Solutions Tab of KeyFile_GWP_Velocity_Exercises.xlsm*

Exercise Set 3

If you have not already downloaded the spreadsheets for the exercises and their solutions that are presented in this book, you can do so at the gw-project.org website on the Groundwater Velocity book page↗ by downloading the interactive Microsoft-Excel spreadsheets titled "**GWP_Velocity_Exercises.xlsm**" and "**KeyFile_GWP_Velocity_Exercises.xlsm**".

Open the spreadsheet "GWP_Velocity_Exercises.xlsm". You may receive a message about enabling content, updating content, or circular references. Proceed by clicking enable content, not updating content, and clicking OK for circular references. Then click on the Exercise 3 tab and look over the interwell tracer test model domain (area in green) as shown in Figure Exercise 3-1. The dispersivities are set to 0.1 m in the flow direction and 0.01 m in the transverse direction.

Above the model domain, the area shaded blue contains three input variables

1) the seepage velocity in m/d
2) the tracer pulse dimension (centered on the injection well) in the flow direction
3) the tracer pulse dimension (centered on the injection well) transverse to flow

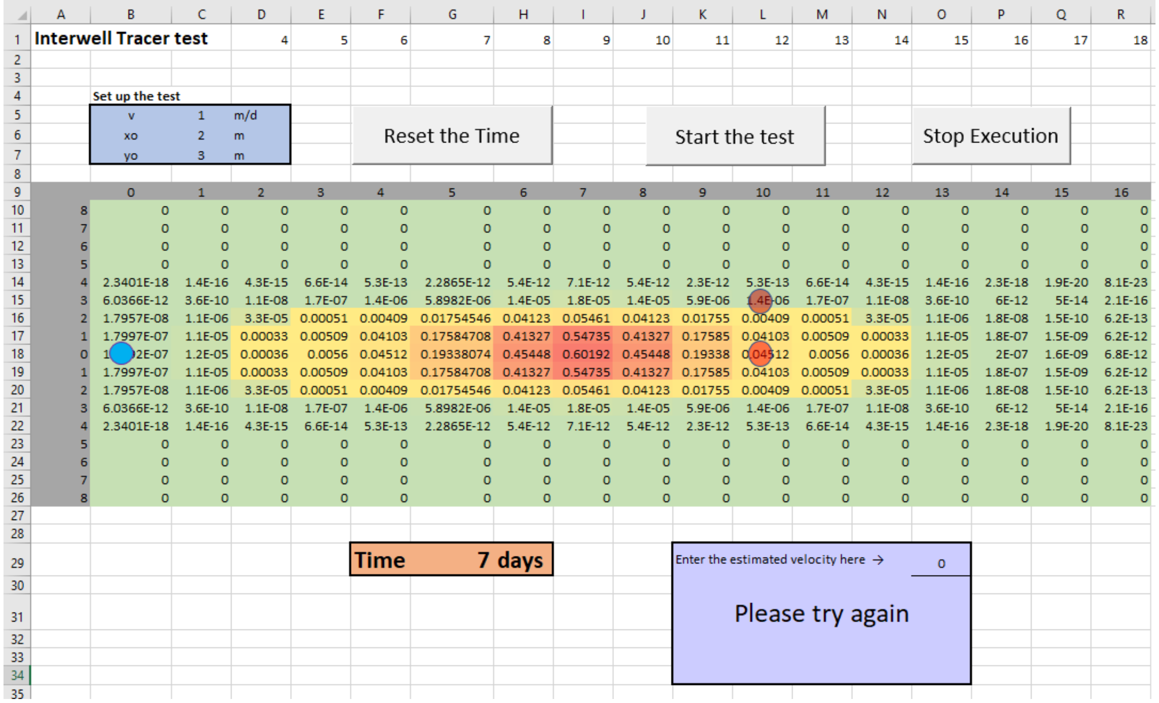

Interwell Tracer test 4 5 6 7 8 9 10 11 12 13 14 15 16 17 18

Set up the test

v 1 m/d
xo 2 m
yo 3 m

	0	1	2	3	4	5	6	7	8	9	10	11	12	13	14	15	16
8	0	0	0	0	0	0	0	0	0	0	0	0	0	0	0	0	0
7	0	0	0	0	0	0	0	0	0	0	0	0	0	0	0	0	0
6	0	0	0	0	0	0	0	0	0	0	0	0	0	0	0	0	0
5	0	0	0	0	0	0	0	0	0	0	0	0	0	0	0	0	0
4	2.3401E-18	1.4E-16	4.3E-15	6.6E-14	5.3E-13	2.2865E-12	5.4E-12	7.1E-12	5.4E-12	2.3E-12	5.3E-13	6.6E-14	4.3E-15	1.4E-16	2.3E-18	1.9E-20	8.1E-23
3	6.0366E-12	3.6E-10	1.1E-08	1.7E-07	1.4E-06	5.8982E-06	1.4E-05	1.8E-05	1.4E-05	5.9E-06	1.4E-06	1.7E-07	1.1E-08	3.6E-10	6E-12	5E-14	2.1E-16
2	1.7957E-08	1.1E-06	3.3E-05	0.00051	0.00409	0.01754546	0.04123	0.05461	0.04123	0.01755	0.00409	0.00051	3.3E-05	1.1E-06	1.8E-08	1.5E-10	6.2E-13
1	1.7997E-07	1.1E-05	0.00033	0.00509	0.04103	0.17584708	0.41327	0.54735	0.41327	0.17585	0.04103	0.00509	0.00033	1.1E-05	1.8E-07	1.5E-09	6.2E-12
0	1[illegible]2E-07	1.2E-05	0.00036	0.0056	0.04512	0.19338074	0.45448	0.60192	0.45448	0.19338	0.04512	0.0056	0.00036	1.2E-05	2E-07	1.6E-09	6.8E-12
1	1.7997E-07	1.1E-05	0.00033	0.00509	0.04103	0.17584708	0.41327	0.54735	0.41327	0.17585	0.04103	0.00509	0.00033	1.1E-05	1.8E-07	1.5E-09	6.2E-12
2	1.7957E-08	1.1E-06	3.3E-05	0.00051	0.00409	0.01754546	0.04123	0.05461	0.04123	0.01755	0.00409	0.00051	3.3E-05	1.1E-06	1.8E-08	1.5E-10	6.2E-13
3	6.0366E-12	3.6E-10	1.1E-08	1.7E-07	1.4E-06	5.8982E-06	1.4E-05	1.8E-05	1.4E-05	5.9E-06	1.4E-06	1.7E-07	1.1E-08	3.6E-10	6E-12	5E-14	2.1E-16
4	2.3401E-18	1.4E-16	4.3E-15	6.6E-14	5.3E-13	2.2865E-12	5.4E-12	7.1E-12	5.4E-12	2.3E-12	5.3E-13	6.6E-14	4.3E-15	1.4E-16	2.3E-18	1.9E-20	8.1E-23
5	0	0	0	0	0	0	0	0	0	0	0	0	0	0	0	0	0
6	0	0	0	0	0	0	0	0	0	0	0	0	0	0	0	0	0
7	0	0	0	0	0	0	0	0	0	0	0	0	0	0	0	0	0
8	0	0	0	0	0	0	0	0	0	0	0	0	0	0	0	0	0

Time 7 days

Enter the estimated velocity here → 0

Please try again

Figure Exercise 3-1 - Model domain and parameters for Exercise Set 3-1

This plume is calculated on a two-dimensional plane assuming a unit thickness in the third dimension (into the page) with uniform conditions throughout the model in that direction.

Three control buttons are provided:

1) 'Reset the time' button that resets the model to initial conditions, at time = 0 days immediately after the tracer is injected.
2) 'Start the test' button to start the clock (and flow) in the test.
3) 'Stop Execution' button suspends the simulation. Once this button is depressed, the test cannot be resumed. A new test must be started by once again pressing the reset button and then the start button.

Beneath the domain is a clock, with bold writing and an orange background. The clock reports the time in days since injection.

To the right of the model domain are two graphs. The upper one shows the concentration of tracer along a line that runs left to right through the middle of the plume at each instant in time. This is a 'profile of the pulse' as shown in Figure Exercise 3-1a. The red dashed line in Figure Exercise 3-1a shows the location of the well on the centerline of the plume. The other graph shows the history of tracer in each of two wells located 10 m from the injection well. One well is on the centerline and the other is off to the side. These graphs of concentration versus time are known as 'breakthrough curves' as shown in Figure Exercise 3-1b.

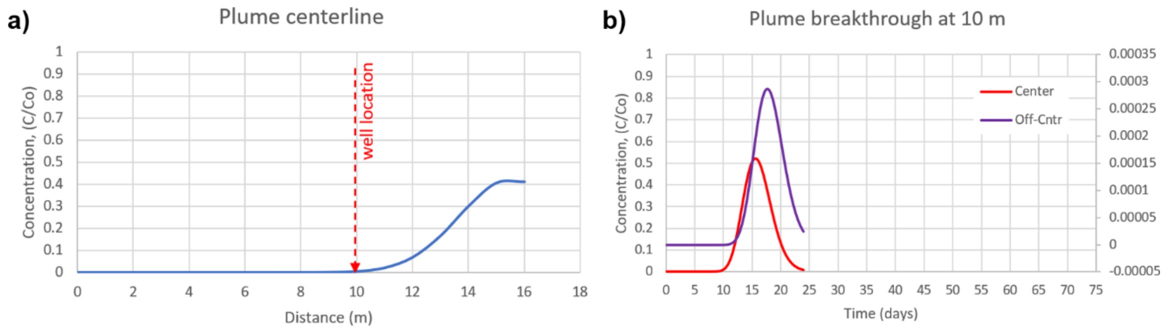

Figure Exercise 3-2 – a) Concentration of tracer along the centerline of the plume at each instant in time which is a 'profile of the pulse' with the red dashed line showing the location of the well. b) Breakthrough curves of concentration in each of two wells located 10 m from the injection well.

<u>Starting an interwell tracer test:</u>

The first time the sheet is accessed, the entry for velocity in the input (blue) area will be blank. This is the correct condition to start a test in which the user must determine a velocity chosen by the sheet. At the end of the test, after the user has pushed the 'stop execution' button, the user's estimate of v can be typed into cell O29 and the sheet will report either "Success!" or "Please try again".

1. If the user wishes to see a test with a particular velocity, then the user-entered value can be typed into cell C5 and the model will run with that velocity.

   To start a test, press "Reset the Time" followed by "Start the test". The tracer will begin its journey from the injection well to the monitoring wells.

   Enter a velocity of 1 m/d into C5 and run a simulation. How many days pass before the peak of the tracer pulse reaches the monitor on the centerline?

   ***The solution for Exercise 3-1** extends from row 169 to row 186 of the Solutions Tab of KeyFile_GWP_Velocity_Exercises.xlsm*

2. Delete the entry in C5 so the velocity input appears to be blank. Reset the time and start the test again.

   This time note the time required for the tracer pulse peak to reach the monitor 10 m away and calculate the groundwater velocity. Enter this value in O29 and determine whether or not your answer is correct.

   ***The solution for Exercise 3-2** extends from row 187 to row 205 of the Solutions Tab of KeyFile_GWP_Velocity_Exercises.xlsm*

3. In Exercise 3-2, the velocity was estimated from the arrival time of the peak. Is this the best part of the curve to use?

   Run tests with input shown in Figure Exercise 3-3 and repeat tests for x_o = 2, 4, and 6 m, effectively changing the source size. Note the arrival time of C = 0.1, C= 0.5 (relative to the maximum concentration that crosses the monitor on the centerline), and the peak and calculate the apparent velocity from each. Which one is closest to the correct value of 1? Explain what is happening here.

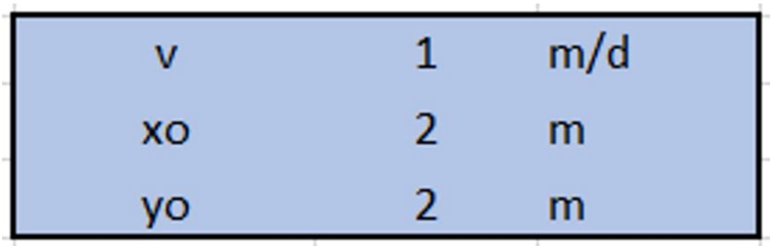

v	1	m/d
xo	2	m
yo	2	m

Figure Exercise 3-3 - Input for the model when undertaking Exercise 3-3.

***The solution for Exercise 3-3** extends from row 206 to row 226 of the Solutions Tab of KeyFile_GWP_Velocity_Exercises.xlsm*

4. If you ran an interwell tracer test with your monitor well not on the centerline, would the velocity estimate be accurate?

Answer this using the breakthrough curve graphs. Run several tests with the input y_o ***varying between 1 m and 8 m and record the velocity determined from each monitor. Type a velocity of 1 m into the v input cell (cell C5) and leave*** x_o ***at 2 m. Run all simulations with this velocity value fixed. Under what conditions are the estimates in best agreement? Worst?***

***The solution for Exercise 3-4** extends from row 230 to row 248 of the Solutions Tab of KeyFile_GWP_Velocity_Exercises.xlsm*

Exercise Set 4

If you have not already downloaded the spreadsheets for the exercises and their solutions that are presented in this book, you can do so at the gw-project.org website on the Groundwater Velocity book page↗ by downloading the interactive Microsoft-Excel spreadsheets titled “**GWP_Velocity_Exercises.xlsm**” and “**KeyFile_GWP_Velocity_Exercises.xlsm**”.

Open the spreadsheet “GWP_Velocity_Exercises.xlsm”. You may receive a message about enabling content, updating content, or circular references. Proceed by clicking enable content, not updating content, and clicking OK for circular references. Then click on the Exercise 4 tab and look over the interface. There are two areas where the user can input parameter values. In the range B4 to C9 is a table where the user can input the x and y coordinates for 5 wells (Figure Exercise 4-1a). These wells will be sampled for water levels - taken from the flow model automatically - and subjected to point velocity determinations, also automatically done by the sheet when prompted by the user.

The second place for user input is in the range R3 to R11. Here the user specifies aspects of the flow model (Figure Exercise 4-1b).

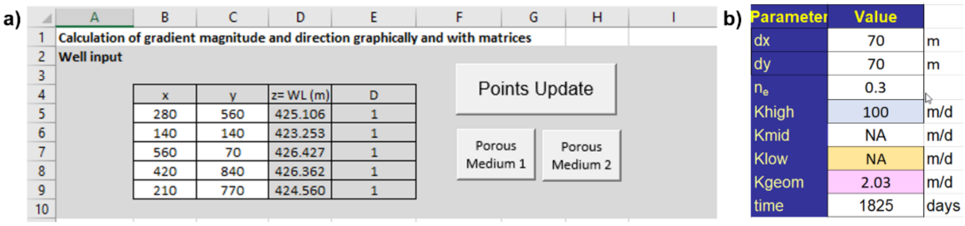

Calculation of gradient magnitude and direction graphically and with matrices

Well input

x	y	z= WL (m)	D
280	560	425.106	1
140	140	423.253	1
560	70	426.427	1
420	840	426.362	1
210	770	424.560	1

Parameter	Value	
dx	70	m
dy	70	m
n_e	0.3	
Khigh	100	m/d
Kmid	NA	m/d
Klow	NA	m/d
Kgeom	2.03	m/d
time	1825	days

Figure Exercise 4-1 - Areas of the “GWP_Velocity_Exercises.xlsm” spreadsheet where the user can vary parameter values of the model. a) Well location coordinates. b) Dispersivities, effective porosity, hydraulic conductivities, and time.

where:

dx = the space between nodes (spreadsheet cells) in the model going left to right

dy = the space between nodes (spreadsheet cells) in the model going up to down

n_e = the effective porosity

Khigh = the hydraulic conductivity of the most permeable sediments

Kmid and *Klow* = available to advanced users, but not active in the default settings

Kgeom = the geometric mean of the hydraulic conductivity in the model domain

time = the time interval used to calculate the velocity vector lengths (for graphics purposes)

Figure Exercise 4-1b lists the default values of these input parameters to be used for the exercises below.

The calculations performed automatically on this sheet are initiated by clicking on the buttons shown in Figure Exercise 4-1a. The Porous Medium 1 and Porous Medium 2 buttons enter two pre-set hydraulic conductivity distributions into the model. These two media are used in the exercises that follow. Users can enter any custom K distribution by simply typing over the K entries in the range R32 to AF46.

The flow system analysis consists of 2 parts: 1) an analysis based on water levels in the 5 wells (Figure Exercise 4-1a) and Darcy's Law; and, 2) point velocity analysis. Both analyses begin by clicking on the Points Update button (Figure Exercise 4-1a).

A user form appears (Figure Exercise 4-2a) when Points Update (Figure Exercise 4-1a) is clicked allowing users to enter well location coordinates manually or automatically. The Autofill option prompts the sheet to randomly select five locations for the wells and enter them into the input table. Calculations begin with the selection of the Calc. Points button (Figure Exercise 4-2a). If the Autofill option is selected, this entails the generation of the random 5 well locations, and the sampling of the flow model for the point velocities, otherwise the manually entered values appear in the Well Input (Figure Exercise 4-1a). The output from this sampling are presented in a table (range B52 to F56, Figure Exercise 4-2b) and a graph (Figure Exercise 4-2c). The graph shows the well locations as orange circles and the direction of flow as blue lines. The lengths of the lines reflect the speed of the water (seepage velocity magnitude). The graph also shows the outcome of the Darcy analysis. This velocity speed and direction is indicated by a large pink circle and rose-colored arrow in the center of the graph.

a)

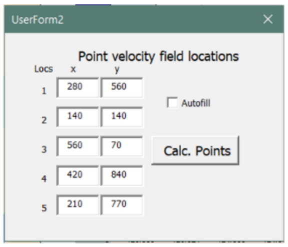

Point velocity field locations

Locs	x	y
1	280	560
2	140	140
3	560	70
4	420	840
5	210	770

b)

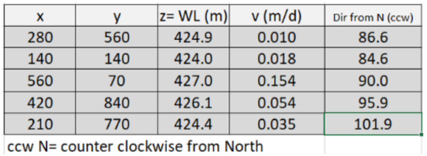

x	y	z= WL (m)	v (m/d)	Dir from N (ccw)
280	560	424.9	0.010	86.6
140	140	424.0	0.018	84.6
560	70	427.0	0.154	90.0
420	840	426.1	0.054	95.9
210	770	424.4	0.035	101.9

ccw N= counter clockwise from North

c)

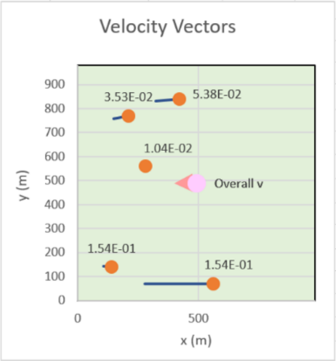

Figure Exercise 4-2 – a) Input well locations. b) Velocity magnitude and direction at each well. c) Location of wells with velocity arrows and overall velocity.

If the user changes the input to the values shown in Figure Exercise 4-1b, the Points Update button must be clicked again, followed by a click of the Calc. Points button to update the results.

A summary of the Darcy and point velocity analyses is presented in the range B29 to D42 (Figure Exercise 4-3a). Selected model inputs are reviewed in the pink area. The results of the matrix analysis (calculated in columns J through O) and Darcy calculations are given in the green area and the point velocity analysis is summarized in the yellow area.

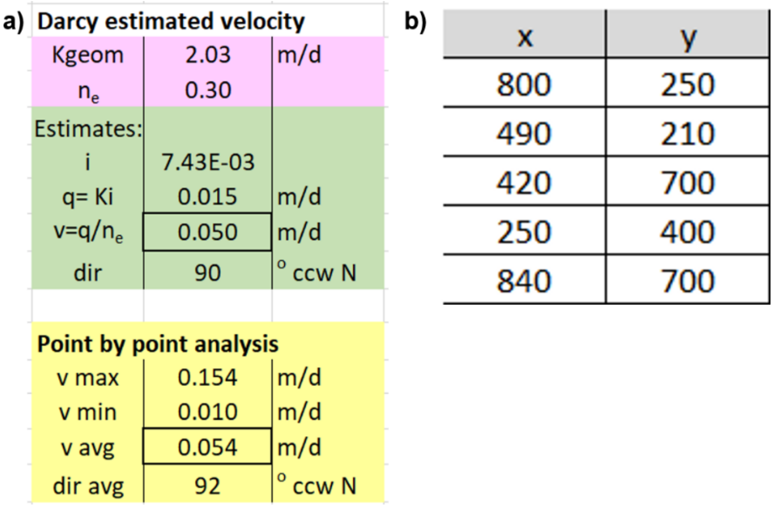

a)

Darcy estimated velocity		
Kgeom	2.03	m/d
n_e	0.30	
Estimates:		
i	7.43E-03	
q= Ki	0.015	m/d
$v=q/n_e$	0.050	m/d
dir	90	° ccw N
Point by point analysis		
v max	0.154	m/d
v min	0.010	m/d
v avg	0.054	m/d
dir avg	92	° ccw N

b)

x	y
800	250
490	210
420	700
250	400
840	700

Figure Exercise 4-3 - Summary of a) the Darcy and point velocity analyses given b) the listed x-y locations of the wells.

1. Input the x, y coordinates shown in Figure Exercise 4-3b into cells B5 to C9 of the Exercise 4 sheet. Make certain the default flow model parameters shown in Figure Exercise 4-1b are correctly entered in range R4 to R11. Click on the Porous Medium 1 button to load that aquifer. Click the Points Update button again, then click the Calc. Points button to update the results.

Compare the Darcy estimate of seepage velocity to the average velocity determined from the point measurements. Compare both the magnitude and direction of average water movement. Next, comment on the range of water speeds and directions identified by the point measurements. Is this variability a concern? Explain why or why not.

***The solution for Exercise 4-1** extends from row 253 to row 282 of the Solutions Tab of KeyFile_GWP_Velocity_Exercises.xlsm*

2. Load Porous Medium 2.

Repeat (1) and extend your answer by contrasting the importance of the velocity variability in the two scenarios and the implications for contaminant transport in these two aquifers.

***The solution for Exercise 4-2** extends from row 284 to row 302 of the Solutions Tab of KeyFile_GWP_Velocity_Exercises.xlsm*

3. For both Porous Medium 1 and Porous Medium 2, Autofill the well location table and fill in the 'Run 1' row in the tables provided in the spreadsheet (cells B71 to H71) based the output in range B29 to D42 in the Exercise 4 sheet (recall Figure Exercise 4-3a). A table is provided from C64 to H68 where you can copy the calculated values for the appropriate run and use paste-special to paste as values into the table below on the appropriate run line. Repeat the Autofill process five times, generating 5 different well location scenarios to fully complete the table for each porous medium.

Investigators often do not know the details of subsurface structures before locating wells. Some well placements may provide representative information that permits reasonable risk assessments. Other well placements may not. Comment on the success or failure of the five well placements summarized in the uncompleted table to the right in the 'Questions' sheet and the box and whisker plots provided immediately below (as completed in the 'Solutions' sheet X305 to AX356 for the data used there).

***The solution for Exercise 4-3** extends from row 305 to row 356 of the Solutions Tab of KeyFile_GWP_Velocity_Exercises.xlsm*

4. ***Comment on the role point velocity measurements might have in contaminant hydrogeological site investigations, based on the results of the simulations above.***

***The solution for Exercise 4-3** extends from row 358 to row 365 of the Solutions Tab of KeyFile_GWP_Velocity_Exercises.xlsm*

7 References

Aley, T, 2002, Groundwater Tracing Handbook. Ozark Underground Laboratory, 1572 Aley Lane, Protem, Missouri, 65733, 35 pages.

Anderson, M.P., 1984, Movement of Contaminants in Groundwater: Groundwater Transport-Advection and Dispersion. Geophysics Study Committee (editors), Studies in Geophysics, National Academy Press, Washington, District of Columbia, USA, pages 37-45.

Ballard, S., 1996, The in situ permeable flow sensor: a ground-water flow velocity meter. Ground Water, volume 34, number 2, pages 231-240.

Ballard, S., G.T. Barker, R.L. Nichols, 1996, A test of the in situ permeable flow sensor at Savannah River, South Carolina, Groundwater, volume 34, number 3, pages 389-396.

Barcelona, M.J., T. Holm, 1991, Oxidation-reduction capacities of aquifer solids. Environmental Science and Technology, volume 25, number 9, pages 1565-1572.

Bedient, P.B., H.S. Rifai, C.J. Newell, 1994, Groundwater contamination, transport and remediation. Prentice-Hall Incorporated, Englewood Cliffs, New Jersey, USA. 542 pages.

Begley, R., 1996, Risk-based remediation guidelines take hold. Environmental Science and Technology, volume 30, number 10, pages. 438A-441A.

Belland-Pelletier, C., M. Fraser, J.F. Barker, T. Ptak, 2011, Estimating contaminant mass discharge: A field comparison of the multilevel point measurement and the integral pumping investigation approaches and their uncertainties. Journal of Contaminant Hydrology, volume 122, pages 63-75.

Bright, J., F. Wang, M. Close, 2002, Influence of the amount of available K data on uncertainty about contaminant transport prediction. Ground Water, volume 40, number 5, pages 529-534.

Brouyere, S., J. Batle-Aguilar, P. Goderniaux, A. Dassargues, 2008, A new tracer technique for monitoring groundwater fluxes: the finite volume point dilution method. Journal of Contaminant Hydrology, volume 95, pages 121-140.

Butler, J.J. Jr., J.M. Healey, 1998, Relationship between pumping-test and slug-test parameters: scale effect or artifact? Ground Water, volume 36, number 2, pages 305-313.

Cherry, J.A., 1990, Groundwater monitoring: some deficiencies and opportunities. Hazardous Waste Site Investigations, Towards Better Decisions, Proceedings of the 10th Oak Ridge National Laboratory Life Sciences Symposium, Gatlinburg, Tennessee, May 21-24.

Clement, T.P., M.J. Truex, B.S. Hooker, 1997, Two-well test method for determining hydraulic properties of aquifers. Ground Water, volume 35, number 4, pages 698-703.

Cook, P., 2020, Introduction to isotopes and environmental tracers as indicators of groundwater flow. The Groundwater Project, Guelph, Ontario, 74 pages.

Crawford, A.J., N.B. Chang, 2016, Developing groundwater variability probes and wireless sensor networks for characterizing the subsurface low flow field. IEEE Sensors Journal, volume 16, number 1, pages 153-162.

Davis, S.N., G.M. Thompson, H.W. Bentley, G. Stilesa, 1980, Ground-water tracers - a short review. Ground Water, volume 18, number 1, pages 14-23.

Devlin, J.F., C.M. McElwee, 2007, Effects of measurement error on horizontal hydraulic gradient estimates in an alluvial aquifer. Groundwater, volume 45, number l, pages 62-73.

Drost, W., 1983, Single well techniques. Tracer Methods *in* Isotope Hydrology. Proceedings of an Advisory Group Meeting Organized by The International Atomic Energy Agency, Vienna, 27 September to 1 October, 1982.

Einarson, M.D., D.M. Mackay, 2001, Predicting impacts of groundwater contamination. Environmental Science and Technology, volume 35, number 3, pages 66A-73A.

Essouayed, E., M.D. Annable, M. Momtbrun, O. Atteia, 2019, An innovative tool for groundwater velocity measurement compared with other tools in laboratory and field tests. Journal of Hydrology X, volume 2, 100008, pages 1-9.

Geyer, T., S. Birk, T. Licha, R. Liedl, M. Sauter, 2007, Multitracer test approach to characterize reactive transport in karst aquifers. Groundwater, volume 45, number 1, pages 36-45.

Gibson, B., J.F. Devlin, 2018, Laboratory validation of a point velocity probe for measuring horizontal flow from any direction. Journal of Contaminant Hydrology, volume 208, pages 10-16.

Gupta, S.K., L.S. Lau, P.S. Moravcik, 1994, Ground-water tracing with injected helium. Ground Water, volume 32, number 1, pages 96-102.

Hatfield, K., M. Annable, J. Cho, P.S.C. Rao, H. Klammler, 2004, A direct passive method for measuring water and contaminant fluxes in porous media. Journal of Contaminant Hydrology, volume 75, pages 155-181.

Kearl, P.M., K. Roemer, 1998, Evaluation of groundwater flow directions in a heterogeneous aquifer using the colloidal borescope. Advances in Environmental Research, volume 2, number 1, pages 12-23.

Keller, C.E., J.A. Cherry, B.L. Parker, 2013, New method for continuous transmissivity profiling in Fractured rock. Groundwater, volume 52, number 3, pages 352-367.

Kerfoot, W.B., V.A. Massard, 1985, Monitoring well screen influences on direct flowmeter measurements. Groundwater Monitoring Review, volume 5, number 4, pages 74-77.

Klammler, H., K. Hatfield, M.A. Newman, J. Cho, M.D. Annable, B.L. Parker, J.A. Cherry, I. Perminova, 2016, A new device for characterizing fracture networks and measuring groundwater and contaminant fluxes in fractured rock aquifers. Water Resources Research, volume 52, pages 5400–5420, doi:10.1002/2015WR018389↗.

Labaky, W., J.F. Devlin, R.W. Gillham, 2007, Probe for measuring groundwater velocity at the centimeter scale. Environmental Science and Technology, volume 41, number 24, pages 8453-8458.

Luhmann, A.J., M.D. Covington, S.C. Alexander, S.Y. Chai, B.F. Schwartz, J.T. Groten, E.C. Alexander Jr., 2012, Comparing conservative and nonconservative tracers in karst and using them to estimate flow path geometry. Journal of Hydrology, volumes 448-449, pages 201-211, doi.org/10.1016/j.jhydrol.2012.04.044↗.

McKay, L.D., W.E. Sanford, J.M. Strong, 2000, Field-scale migration of colloidal tracers in a fractured shale saprolite. Ground Water, volume 38, number 1, pages 139-147.

McNab, W.W., B.P. Dooher, 1998, A critique of a steady-state analytical method for estimating contaminant degradation rates. Ground Water, volume 36, number 6, pages 983-987.

Morris, D.A., A. I. Johnson, 1967, Summary of hydrologic and physical properties of rock and soil materials, as analyzed by the Hydrologic Laboratory of the U.S. Geological Survey, 1948-60. Geological Survey Water-Supply Paper 1839--D, United States Government Printing Office, Washington, 42 pages.

Osorno, T., J.F. Devlin, 2018, An in-well point velocity probe for the rapid characterization of groundwater velocity at the centimeter-scale. Journal of Hydrology, volume 557, pages 539-546.

Pehme, P.E., B.L. Parker, J.A. Cherry, J.P. Greenhouse, 2010, Improved resolution of ambient flow through fractured rock with temperature logs. Ground Water, volume 48, number 2, pages 191-205.

Post, V., J.R. von Asmuth, 2013, Review: Hydraulic head measurements—new technologies, classic pitfalls. Hydrogeology Journal, volume 21, pages 737–750.

Rifai, H.S., and P.B. Bedient, 1990, Comparison of biodegradation kinetics with an instantaneous reaction model for groundwater. Water Resources Research, volume 26, number 4, pages 637-645.

Sale, T., Gallo, S., Askarani, K.K., Irianni-Renno, M., Lyverse, M., Jopkins, H., Blotevogel, J., Burge, S. 2020. Real-time soil and groundwater monitoring via spatial and temporal resolution of biogeochemical potentials. Journal of Hazardous Materials. accesses at https://doi.org/10.1016/j.jhazmat.2020.124403, November 26, 2020.

Schillig, P., J.F. Devlin, M. McGlashan, G. Tsoflias, J.A. Roberts, 2011, Transient heterogeneity in an aquifer undergoing bioremediation of hydrocarbons. Ground Water, volume 49, number 2, pages 184-196.

Sterling, S.N., B.L. Parker, J.A. Cherry, J.H. Williams, J.W. Lane, F.P. Haeni, 2005, Vertical cross contamination of trichloroethylene in a borehole in fractured sandstone. Ground Water, volume 43, number 4, pages 557-573.

Su, G.W., B.M. Freifeld, C.M. Oldenburg, P.D. Jordan, P.F. Daley, 2006, Interpreting velocities from heat-based flow sensors by numerical simulation. Ground Water, volume 44, number 3, pages 386-393.

Sudicky, E.A., and J.A. Cherry, 1979, Field observations of tracer dispersion under natural flow conditions in an unconfined sandy aquifer. Water Pollution Research Journal of Canada, volume 14, pages 1-17.

van der Kamp, G., 1992, Evaluating the effects of fractures on solute transport through fractured clayey aquitards. Proceedings of the 1992 Conference of the International Association of Hydrogeologists, Canadian National Chapter, Hamilton, Ontario, May, 9 pages.

Vulava, V.M., E. B. Perry, C.S. Romanek, J.C. Seaman, 2002, Dissolved gases as partitioning tracers for determination of hydrogeological parameters. Environmental Science and Technology, volume 36, number 2, pages 254-262.

8 Exercise Solutions

A spreadsheet for conducting the exercises “**GWP_Velocity_Exercises.xlsm**” and a spreadsheet providing their solutions “**KeyFile_GWP_Velocity_Exercises.xlsm**” can be downloaded from the Groundwater Velocity book page↗ at the gw-project.org website.

9 About the Author

Dr. J.F. Devlin is a Professor in the Geology Department at the University of Kansas, USA, and previously served on the faculty of the University of Waterloo. He has 35 years of experience in the groundwater field, has supervised 35 student theses and published 75 peer reviewed articles in groundwater research. He has worked collaboratively with academic and government researchers in the USA, Canada, France, Denmark, and New Zealand. He has also worked jointly with industrial partners in North America and Europe. His research interests range from organic contaminant geochemistry to aquifer characterization, bioremediation, subsurface mixing in groundwater remediation schemes, and the direct measurement of groundwater velocity. He currently serves on the Board of the Tumbling Creek Cave Foundation and has served as an Associate Editor for Groundwater Monitoring and Remediation and the Hydrogeology Journal and as Editor-in-Chief for Groundwater Monitoring and Remediation. He the recipient of the W.B. Pearson Medal from the University of Waterloo, an NSF Career Award, the Otto Monsted guest professorship at DTU, Leo M. & Robert M. Orth Water Resources Award and a Kemper Award for teaching excellence.

Please consider signing up to the Groundwater Project mailing list and stay informed about new book releases, events and ways to participate in the Groundwater Project. When you sign up to our email list it helps us build a global groundwater community. Sign-up↗.

THE
GROUNDWATER
PROJECT

Modifications from original release

page 10, 2nd to last line of the caption to Figure 6, the font of “t2” was changed to italic.

page 20, 3rd line above Figure 15: $t^{½}$ was changed to t½.

page 33, the figure reference was changed from 11 to 24 in the phrase: “such as the one illustrated in Figure 11” to “such as the one illustrated in Figure 24”

page 33, caption to Figure 25 the font of Cwell and MD was changed to italic.

page 52, part 3 of Exercise Set 3, Figure number 3-2 was changed to 3-3 in both the text and figure caption.